GD/C-DBE66-006
Space Science Laboratory

General Dynamics Corporation
Convair Division
P. O. Box 1128
San Diego, California 92112

STUDY ON THE SPECTRAL EMISSIVITY OF CARBON PARTICLES PRODUCED BY A ROCKET MOTOR

FINAL REPORT

CONTRACT NAS 8-11455
Control Number: DCN 1-4-75-01094-01, S1 (1F)
Type of Contract: Cost-Plus-A-Fixed Fee

MAY 1966

GENERAL DYNAMICS CONVAIR

STUDY ON THE SPECTRAL EMISSIVITY OF CARBON PARTICLES PRODUCED BY A ROCKET MOTOR

FINAL REPORT

MAY 1966

This report was prepared by General Dynamics Corporation, Convair Division, under Contract NAS 8-11455, "Continuum Carbon Emission for Afterburning Studies," for the George C. Marshall Space Flight Center of the National Aeronautics and Space Administration. The work was administered under the technical direction of the Aero-Astrodynamics Laboratory (R-AERO-R) of the George C. Marshall Space Flight Center with R. M. Huffaker acting as project monitor.

TABLE OF CONTENTS

LIST OF FIGURES

LIST OF FIGURES (CON'T)

LIST OF FIGURES (CON'T)

SUMMARY

This report documents research performed for NASA-MSFC uncer Contract NAS 8-11455 between 1 July 1964 and 30 April 1966. Research was performed to evaluate the spectral emissivity of clouds of very small carbon particles present in the exhaust plumes of rocket engines using oxygen and RP-1 propellants, for the purpose of developing methods of analyzing and predicting radiative base heating on the Saturn V and other large launch vehicles. Scientific and technical personnel who spent appreciable time on this study were C. C. Ferriso (principal investigator and project leader up to the time of his death on 31 January 1966), C. B. Ludwig (principal investigator and project leader from 1 February 1966), F. P. Boynton, A. Thomson, L. Acton, D. Brewer, C. N. Abeyta, and D. Suttie. The contract monitor was R. M. Huffaker, Aerodynamics Branch, NASA-MSFC.

The purpose of the present study was to measure the wavelength and temperature dependence of the absorption coefficient of the cloud of solid carbon or soot particles produced by the combustion of RP-1 with GO_2 in small research rocket motors. At the equivalence ratios at which full scale engines operate, and at the equivalence ratios used in this study, the carbon is a nonequilibrium product of the sooty flame in the combustion chamber. The amount produced depends on the combustion conditions, and cannot be quantitatively predicted. The engines used in this study were designed for high combustion efficiencies. The amount of carbon produced by them was much less, at similar O/F ratios, than that of typical operational engines. This is presumably due to their greater mixing efficiency, greater chamber length, or the use of GO_2 rather than LO_2. The amount

of carbon produced was found to decrease rapidly with increasing O/F ratio (to mass fractions < 0.05% at O/F ratios ≥ 2.2) and to increase significantly with chamber pressure. (In a separate experiment performed by Rocketdyne with a standard Atlas vernier engine the amount of carbon produced was found to be relatively insensitive to O/F ratios between 1.7 and 2.7.)

Another effect important to the base heat transfer is associated with the thermochemistry of carbon formation. When a significant amount of carbon is produced the temperature of the gases at the exit plane increases and can exceed the chemical equilibrium value. Since carbon tends to dominate the radiant heat transfer from RP-1/O_2 propellant systems, these observations indicate a strong correlation between combustion chamber design and the level of radiant heat transfer due to solid carbon. The general tendency to use as short a chamber and as high a chamber pressure as possible to get high performance seems to favor carbon formation and thus to raise the level of the base radiant heat transfer. This conclusion may not be of much practical importance, since the level of the base radiant heat transfer has not usually been considered a significant factor in the design of operational motors.

In establishing an approach to the present problem, we have assumed (for the reasons just described) that it will be necessary, in order to evaluate radiant heat transfer, to measure the amount of carbon formed in the full scale engines as a function of position in the flow field. Since the particles produced appear to be of small size, it appears adequate to

measure only the mass density of the carbon particle cloud at one point on each streamline sufficiently removed from the combustion chamber that subsequent chemical reactions may be neglected. The particles may then be assumed to follow the gas streamline through the remainder of the flow. This latter assumption may fail in portions of the flow field where the gas density is low and the streamline curvatures are large. In this case it would be necessary to know also the distribution of particle sizes. However, the sizes that we have observed are sufficiently small that this effect is not expected to be significant in the region downstream of the exit plane. Also, because of the small particle sizes, the optical scattering coefficients are expected to be negligibly small at the wavelengths for which heat transfer is important ($> 1\ \mu$).

The most convenient point to measure the carbon concentration is at the nozzle exit plane. Two methods for measuring the carbon concentration have been considered: 1) direct measurement of the carbon flux with a probe inserted into the flow and 2) deduction of the radial carbon concentration profile from measurements of the radiance and/or transmission across the nozzle exit as a function of displacement of the line of sight from the nozzle centerline. The second method has the distinct advantage that absolute values for the absorption coefficient are not required for the subsequent determination of the radiant heat transfer to the base - only the relative spectral and temperature dependencies. Thus any experimental errors in the determination of the absolute carbon mass flux, either in the small or full scale engines, cancel out. If both transmission and radiance measurements are made, one obtains in addition the actual tempera-

ture profile at the exit plane and can thus account for any chemical non-equilibrium effects realistically. However, the rather high absorptivities of the gas at short wavelengths, the interfering effects of molecular absorption, and the sharp gradients expected near the nozzle edge (due to the boundary layer and the exhausterator) limit the accuracy of this method. In practice a combination of both methods is probably necessary.

In the present study we have attempted to measure the relative dependence of the spectral absorption coefficient on wavelength and temperature in the region between 1 and 4 μ. No attempt to measure directly the carbon mass fraction was made. Theoretical calculations of the absorption coefficient were used to relate the measured emissivities to absolute absorption coefficients. The spectral emissivity at the exit plane of various small RP-1/O_2 rocket motors designed to yield uniform exit flow (Foelsch nozzles) was measured as a function of wavelength at various O/F ratios. The temperature dependence was obtained by expanding the combustion products generated at fixed O/F ratio and chamber pressure in identical combustion chambers to different area ratios, thereby producing a given amount of carbon at different temperatures. The exit plane temperature was measured by an emission-transmission technique (usually in the 4.3-μ band of CO_2); the spectral emissivity of the combustion products was determined from the measured temperature and spectral radiance. Subtraction of the molecular contribution then yielded the product of carbon absorption coefficient and carbon mass density at wavelengths between 1 and 4 μ and temperatures between 1000° and 2600°K. For temperatures below 1700°K, the spectral dependence of k_λ is in reasonably good agreement with a theoretical calculation based on the dc conductivity of bulk

carbon and appropriate to very small particles. Setting k_λ proportional to λ^{-1} and independent of temperature is also consistent with the present data below 1700°K. However, for temperatures well above 1700°K, the wavelength dependence of k_λ was markedly different from the theoretical estimates and becomes almost independent of wavelength. The temperature dependence at the higher temperatures was also significantly different from the theoretical estimates.

The difference between the measured and calculated absorption coefficients at high temperatures is not unexpected, since the properties of these carbon particles could be quite different from those of the bulk material. However, we have used the theoretical calculations to normalize the present observation because of the agreement of the spectral dependence of absorption coefficients (as well as one measurement of this absolute magnitude) of soots extracted from flames with the calculations. At temperatures above 1700°K absolute (normalized) values of k_λ were determined by demanding agreement between experiment and calculation at 2.2 μ. Thus, although absolute values are tabulated in Table II, it is only the relative variation with wavelength and temperature which were measured; the tabulated values actually contain a normalizing factor which has not been measured.

The determination of the temperature dependence was not as accurate as had been originally hoped. The high sensitivity of the amount of carbon formed to slight variations in the operating mixture ratio made it quite difficult to ensure that measurements made with the different area ratio engines were obtained at precisely the same carbon mass fraction. The uncertainties of the present data imply that, for scaling a measurement

made at a typical exit temperature of 1600°K down to 1000°K or up to 2600°K, the uncertainty in the absorption coefficient at these limits may be as large as ± 50%. The uncertainty in the wavelength dependence based on the present measurements alone results principally from errors in measuring the temperature. Since the measurements were made principally in emission, the deduced emissivity at wavelength λ is as uncertain as is the ratio of the Planck function at λ to that at the wavelength where the temperature determination was made (usually near 4 μ). At temperatures about 2300°K the uncertainty in scaling a measurement made at 4.0 μ to 1 μ is about ± 25%. At lower temperatures the errors can be larger: e.g., at about 1200°K the uncertainty in scaling from 4 μ to 2 μ is about 25% and to 1 μ about ± 50%.

INTRODUCTION

A recurring and serious problem in launch vehicle development is the severe convective and radiative heating of the base region by the vehicle's exhaust gases. Heat is transferred from the exhaust to the base by radiation and convection, and under some circumstances the radiative contribution is comparable to the convective.[1] It is difficult to predict base heating for vehicle systems different from those on which large amounts of flight data exist. Model tests, for example, involve very complicated scaling problems[2,3] when one attempts to extrapolate their results to the full-scale situation. From radiative heat fluxes measured as a function of altitude at a point on the base of the Saturn SA-4 flight vehicle and on wind tunnel models,* one could conclude that the model and full-scale radiative fluxes are the same. It is doubtful that one would have predicted this result, or that it can be taken as a general rule.

Development of reliable procedures of predicting base heating requires a knowledge of the flow field, of the exhaust chemistry, and of the emissive properties of the radiating species. When the vehicle burns a hydrocarbon fuel with oxygen, the radiation to the base is primarily due to emission from CO_2, H_2O, and solid carbon or soot. Molecular emission at the temperatures of interest (1000°-3000°K) is restricted to the various vibration-rotation bands and has a complex frequency dependence. The solid carbon, on the other hand, gives rise to a continuous and smoothly varying spectrum. Water and carbon dioxide are equilibrium products of combustion;

*This information was kindly furnished to us by Mr. Homer Wilson of NASA-MSFC.

solid carbon is not. Thermodynamic calculations predict no solid carbon for the normal operating mixture ratios (O/F = 2.3 to 2.6). Some fuels, such as alcohol and certain hydrazine derivatives, appear to produce little or no carbon when burned in rocket engines.

An estimate of the relative importance of the different radiating species may be obtained from an examination of available total hemispherical emissivity data for conditions characteristic of an exhaust plume. In Figs. 1 and 2 we have plotted the total emissivities for each species versus pathlength. The molecular data were taken from Hottel's charts.[4] The carbon data were taken from a calculation which will be described subsequently. The carbon mass fraction was deduced from measurements of the spectral radiance of an Atlas booster engine.[5] These figures show that, for the thick optical paths of interest for Saturn-class vehicles, carbon may contribute more than fifty percent of the total emission. The work reported here concerns the experimental determination of the absorption coefficients for carbon produced by an RP-1/oxygen rocket engine, and the comparison of these data with theoretical predictions.

The properties of carbon or soot in flames have been studied extensively. Several reviews concerning the formation, combustion, and radiative properties of soot in laboratory flames are available.[6,7] As yet, the formation mechanism is poorly understood. Gasification of soot by endothermic reactions with H_2O or CO_2 is apparently slow at the temperatures in most flames. Combustion with oxygen is known to be rapid when the particle temperature exceeds an ignition value of the order of 800°C.[8] Flame soot particle sizes[9] generally range from 50 Å to 500 Å.

Hottel[4] has collected and correlated much of the older data on the

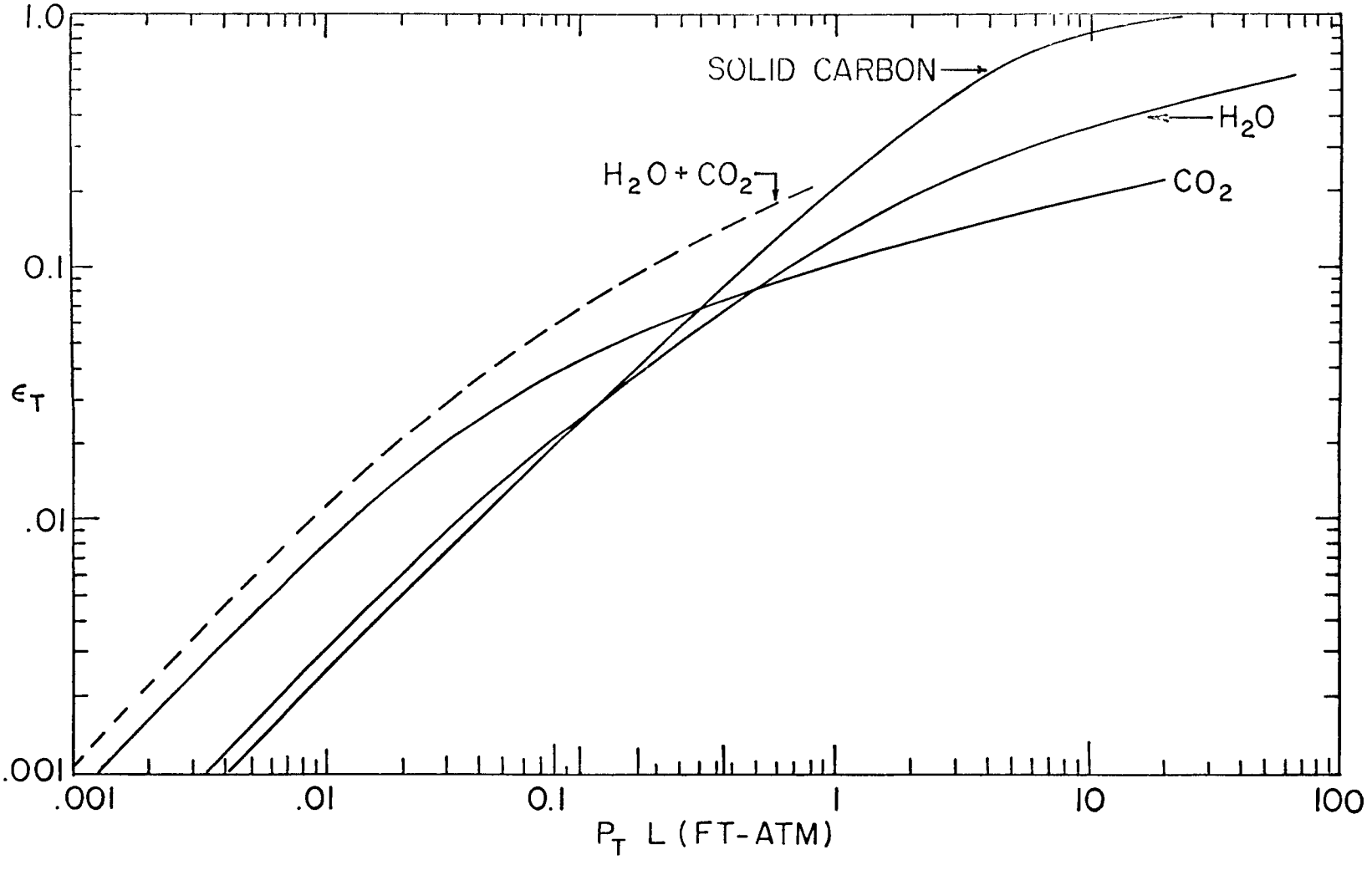

Figure 1. Total emissivities in a RP-1/O_2 afterburning flame at 1000°K; composition is 30 mole % H_2O, 20 mole % CO_2, 0.4 mass % solid carbon; no pressure correction made for molecular emitters.

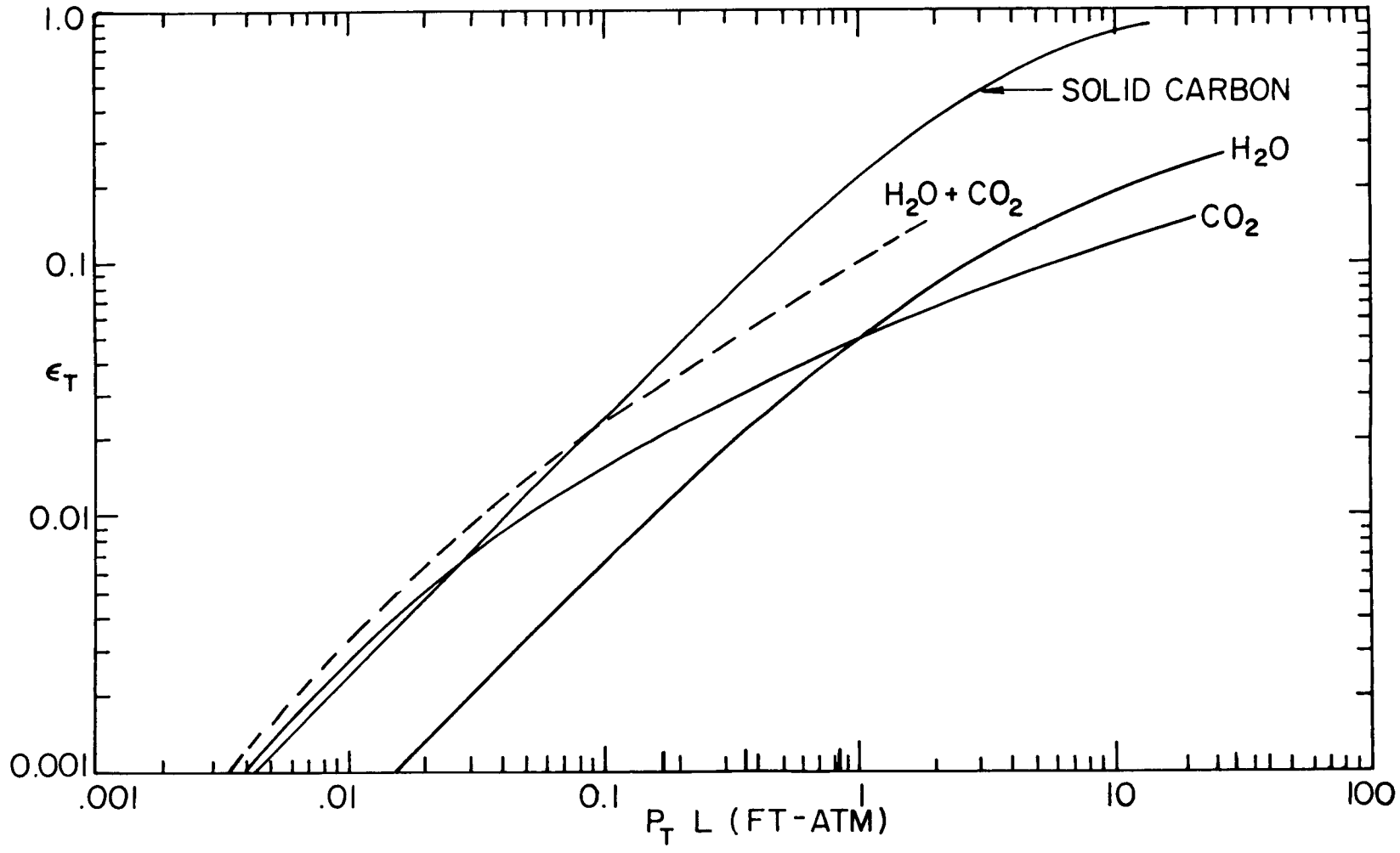

Figure 2. Total emissivities in a RP-1/O_2 afterburning flame at 2000°K; composition as in Figure 1.

optical properties of soot in flames. Since the actual carbon mass fraction is difficult to measure, much of the information is in the form of relative spectral data. Siddall and McGrath[10] give relative measurements of the absorption coefficients of soots from various flames. Foster[11] has reported some absolute measurements of soot absorption coefficients. Theoretical values for the absorption and scattering coefficients of clouds of dispersed carbon particles have been computed[12] from the properties of carbon in bulk form. Much of the available experimental data is obtained for soot that has been extracted from the flame, and therefore represents the absorption properties at room temperature. Some measurements in situ indicate that, in the visible and near infrared, the spectral distribution is similar to that of the extracted soot.

A number of measurements of rocket exhaust emission are available (some only in classified reports); from these, one can determine some apparent properties of the carbon produced by rockets. Simmons[13] has measured the radiance and emissivity over limited spectral regions in the visible and infrared at the exit of a modified Atlas vernier engine burning RP-1 and LO_2 at various O/F ratios. The continuum absorption coefficient, which we deduced from his data, has a distinctly different wavelength dependence in the visible region than the flame data. DeBell and Speiser[5] measured the spectral radiance at the exit plane of an Atlas booster engine. Using calculated exit plane temperature and density profiles we evaluated the expected radiance spectrum both for the flame-type absorption coefficients and for values inferred from the vernier engine data. The value of the carbon concentration was adjusted to give good agreement at 2.2 μ, a molecular spectral "window"; we found that both calculations predicted

exit plane spectral radiancies which were consistent within the scatter of the data at all wavelengths longer than 1.0 μ. In the near infrared and visible, however, only the vernier engine values gave reasonable correlation.

The present spectral radiance measurements agree qualitatively with Simmons' measurements at wavelengths greater than 1 μ. For reasons to be discussed subsequently, a comparison at short wavelengths is not possible. There is a striking difference between the dependence of carbon emissivity on O/F ratio in the two measurements: over the same O/F ratio for which Simmons' measurements showed less than a 50% change in emissivity, ours show more than an order of magnitude change. This difference indicates the importance of the combustion conditions on the level of the carbon emissivity in a rocket exhaust.

THEORETICAL CALCULATIONS

Stull and Plass[12] have calculated the absorption and scattering coefficients for dispersed carbon particles at 2250°K from the Mie theory using the electrical properties of carbon in bulk form. In the present experiment, the particle size is very small compared to the wavelength in the spectral range of interest ($\lambda > 1.0\ \mu$). Thus the extinction due to scattering may be neglected compared to that due to absorption, and the absorption coefficient per unit mass of the particle cloud becomes independent of the particle size. In this limit and at wavelengths greater than 1 μ, the calculations of Stull and Plass may be easily extended to cover the temperature range of interest.

Following Siddall and McGrath,[10] we may express the linear absorption coefficient in the form

$$k = 36\pi\rho F(\lambda)/\rho_o\lambda\ , \tag{1}$$

where ρ is the carbon particle mass density (gms/cm^3 of cloud), ρ_o is the density in bulk form and λ the wavelength. The function $F(\lambda)$ is related to the complex index of refraction $N_1(1-iN_2)$ by the expression

$$F(\lambda) = \frac{N_1^2 N_2}{(N_1^2+N_1^2N_2^2)^2 + 4(N_1^2-N_1^2N_2^2+1)}\ . \tag{2}$$

Stull and Plass give general expressions for N_1 and N_2. They are

$$N_1^2 - N_1^2N_2^2 = 1 + \frac{e^2}{m\epsilon_o}\sum_j \frac{n_j(\omega_{o_j}^2-\omega^2)}{(\omega_{o_j}^2-\omega^2)^2 + \omega^2 g_j^2} - \frac{n_c}{\omega^2+g_c^2} \tag{3}$$

and

$$2N_1^2N_2 = \frac{e^2}{m\epsilon_o} \sum_j \frac{n_j \omega g_j}{(\omega_{o_j}^2 - \omega^2)^2 + \omega^2 g_j^2} + \frac{n_c g_c}{\omega(g_c^2 + \omega^2)}, \tag{4}$$

where n_c = number of conduction electrons/cm^3, g_c = damping constant for conduction electrons, n_j = number of bound electrons in the jth state per cm^3, ω_{o_j} = natural (circular) frequency of the jth state, g_j = damping constant for the jth state and ω = circular frequency of the radiation. Stull and Plass give values for the various constants at 2250°K evaluated from the measurements of Senftleben and **Benedikt.**[14]

At wavelengths greater than about 1 μ, these expressions may be approximated by

$$N_1^2 - N_1^2N_2^2 \simeq 4.36 - 1.31 \frac{\gamma}{\beta^2} \tag{5}$$

$$N_1^2N_2 \simeq \frac{0.58}{\lambda} + \frac{1.675\lambda}{\beta} \tag{6}$$

where

$$\beta = \sigma_{dc}(2250°K)/\sigma_{dc}(T),$$

$$\gamma = n_c(2250°K)/n_c(T),$$

$$\sigma_{dc} = e^2 n_c/m\epsilon_o \mu g_c,$$

and λ is the wavelength in microns. These expressions have been used to evaluate the carbon cloud absorption coefficients. Measured values of the variation of the dc conductivity of bulk carbon with temperature were used to evaluate the ratio β. The results are relatively insensitive to the

temperature dependence of the factor γ at temperatures between 500° and 2500°K and at wavelengths greater than 1 μ. In the actual calculation, γ was set equal to unity. The results are shown in Fig. 3, where the parameter $k\lambda/\rho$ is plotted as a function of λ for various temperatures. A comparison with the measurements collected by Hottel is shown in Fig. 4.

Since the calculated absorption coefficients are based on the properties of carbon in bulk form, it is not obvious a priori that these should necessarily represent those of carbon formed by flames, especially since the infrared absorptive properties are principally dependent on the properties of the conduction electrons. The comparisons of the calculated absorptive properties with the flame data indicate that, within the experimental uncertainties, the variation with wavelength is reasonably well reproduced. Nevertheless, this agreement should not be construed as an indication that the absolute value of the absorption coefficients will show similar agreement.

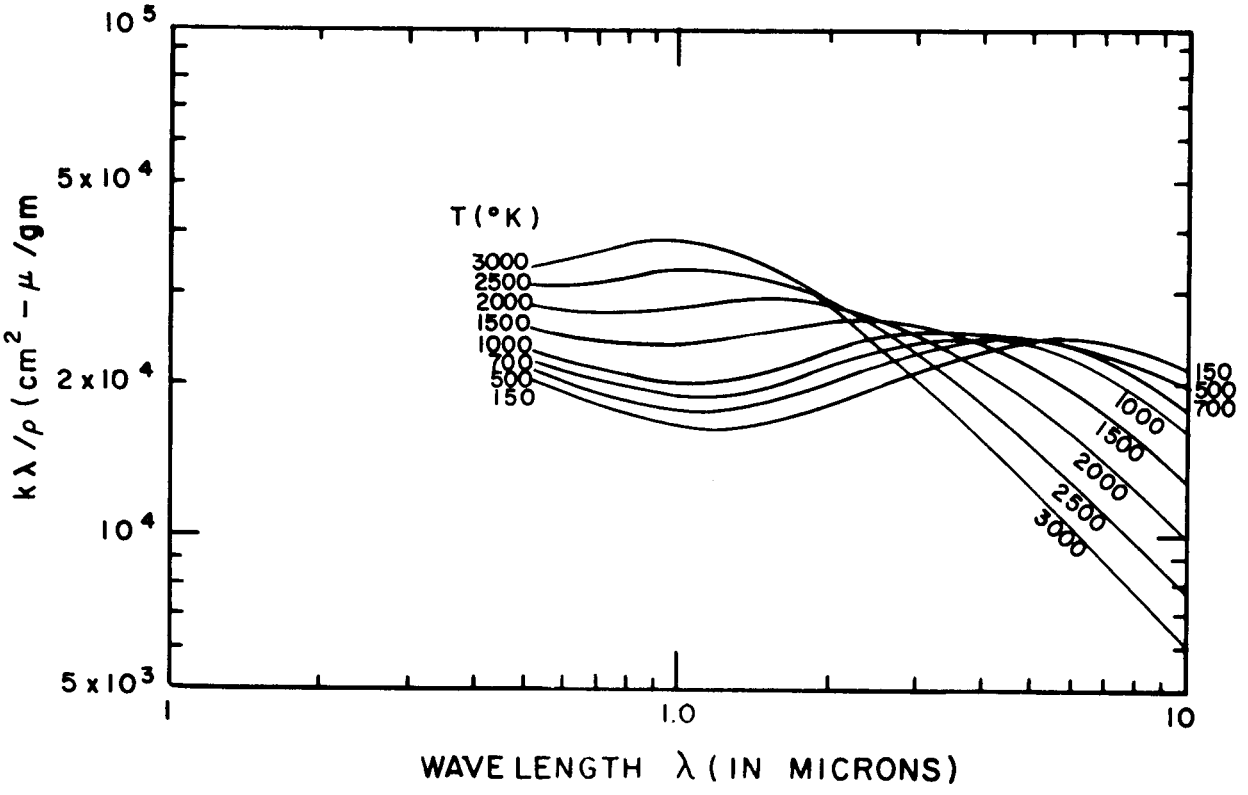

Figure 3. Linear absorption coefficient for clouds of very small carbon particles.

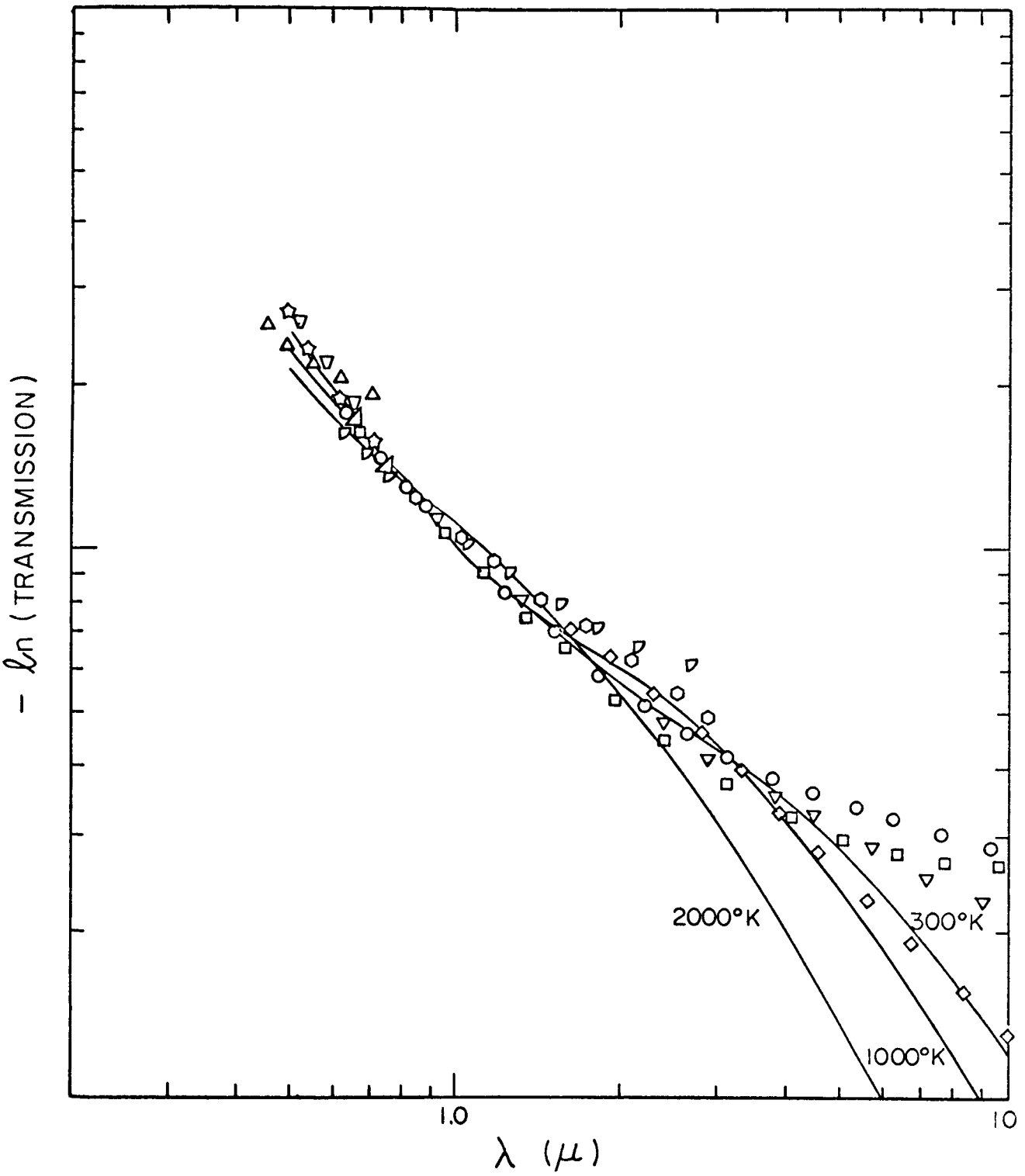

Figure 4. Comparison of experimental and calculated transmission data for soot layers and carbon particles in flames. Experimental points from Ref. 4. Calculated curves adjusted to coincide at 0.8 μ.

EXPERIMENTAL MEASUREMENTS OF CARBON PARTICLE EMISSION

Because the carbon emission spectrum varies slowly with wavelength, Beer's law applies to transmission or emission measurements made at moderately low spectral resolution. Thus, measurements on thin samples of carbon-bearing gas may be reliably extrapolated to any desired thickness. In comparison with molecular emission, the experimental problem is greatly simplified: only the temperature, and not pathlength or pressure, need be varied to obtain the emissive properties of a given sample under all conditions where scattering is unimportant.

The present experiment is quite similar to that in which Ferriso and Ludwig[15] measured emissivities of hot CO_2 and H_2O. A small rocket motor is used to generate the observed gas sample, and measurements are made as close as possible to the exit plane. This apparatus has been described in detail elsewhere. In the present work the motors burned RP-1 and GO_2. The operating conditions (chamber pressure and propellant mass flow vs mixture ratio) are shown in Figs. 5 and 6. Measurements of spectral emissivity were obtained in the wavelength range from 5 to 0.7 μ, and at temperatures between 1000° and 2600°K. Three motors were used in this study, with identical injectors, combustion chambers, and nozzle contours upstream from the throat section. The diverging sections were different; combustion products were expanded in contoured nozzles designed by Foelsch's method[16] to area ratios of 5.25, 3.0, and 1.5. The first nozzle produces a fully expanded jet at 1.0 atm exit pressure when operated at chamber pressures between 370 and 520 psia, depending on O/F ratio. The other engines are underexpanded when operated at the same chamber conditions, producing higher exit plane temperatures. The O/F ratio in this study was varied between 1.2 and 2.0.

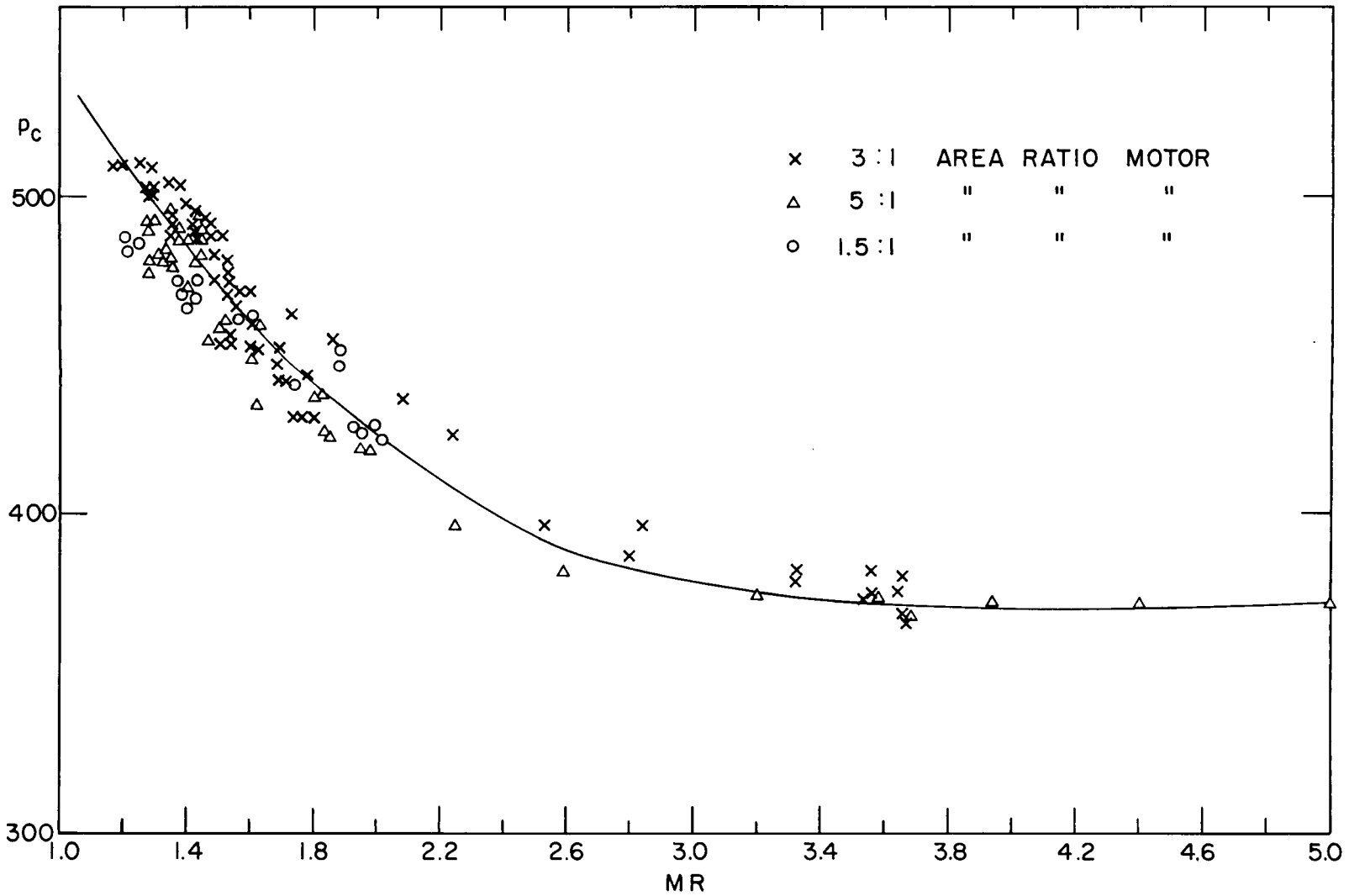

Figure 5. Chamber pressure (psia) versus O/F ratio for the three engines.

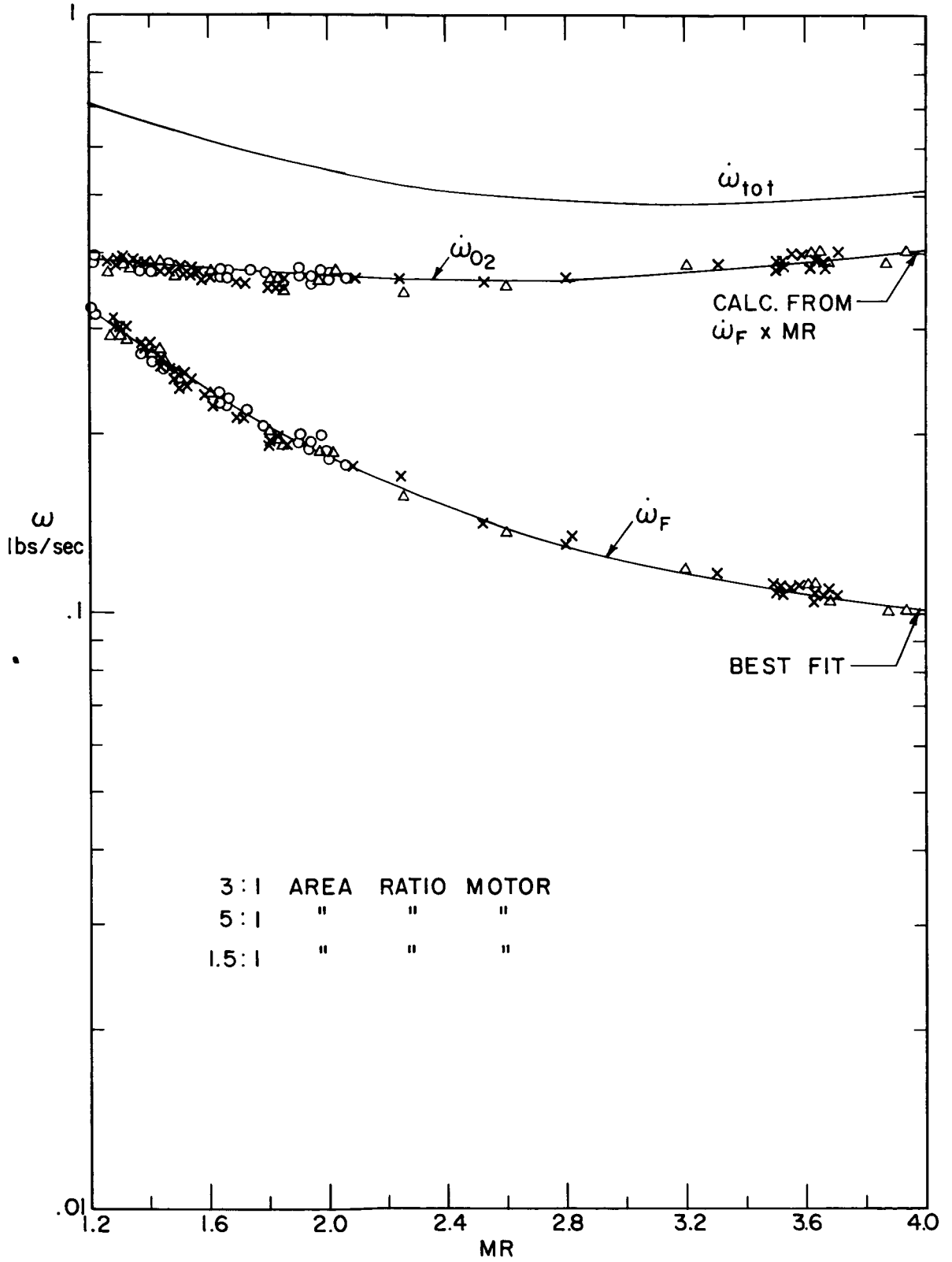

Figure 6. Propellant mass flow versus O/F ratio for the three engines.

When any one of these motors is operated at different times with the same nominal chamber conditions, the continuum emission level is reasonably reproducible. There is some scatter, which we attribute to the difficulty of producing exactly the same flow rates. This behavior implies that the carbon particle mass fraction is reproducible in this motor. Since all of the motors are identical upstream of the throat, the amount of carbon produced at the throat section of one motor should be the same as that produced at the throat of another, when O/F ratio and P_c are held constant. Any difference in carbon mass fractions or size between our motors is therefore caused by effects downstream of the throat.

In the diverging section of the nozzle, we expect that particles may grow by agglomeration or shrink through gasification. The only rapid gasification process is reaction with O_2 or O. In Table I, the calculated equilibrium chamber mole fractions of O and O_2 are tabulated at several O/F ratios. The rates of 2- and 3-body reactions are known to be fast enough to maintain equilibrium upstream of the throat section of these nozzles, and therefore we would expect these mole fractions to exist in the chamber provided that the propellants are fully mixed. In lean regions, the mole fractions of O and O_2 will be higher than those shown in Table I; in rich regions, where the carbon particles are presumably formed, the amounts of O and O_2 will be less. Recombination in the upstream regions of the nozzle will reduce these mole fractions by factors ≥ 10. A particle of 250 Å radius (containing between 10^6 and 10^7 atoms, depending on how densely packed the particle is), passing through the diverging section of the nozzle, suffers at most about 3×10^4 collisions with O and O_2 molecules. Therefore, even if every collision were effective, a negligible amount of the particle mass could

disappear by reaction in the diverging section even if perfect mixing were achieved.

Table I: Equilibrium chamber mole fractions

O/F ratio	x_O	x_{O_2}
1.2	$< 10^{-10}$	$< 10^{-10}$
1.4	1×10^{-7}	1×10^{-8}
1.6	2×10^{-5}	3×10^{-6}
1.8	3×10^{-4}	1×10^{-4}

The effects of agglomeration are more difficult to determine accurately. If the particles were to collide under the influence of Brownian motion,[17] and if every collision were to result in "sticking" of the two particles, then when there are 10^{10} particles/cm^3 of 250 A radius (corresponding to a carbon mass fraction of 1%) about 10^3 of them per cm^3 will coagulate during their passage through the diverging section. This coagulation rate is small enough to be negligible. Other effects, such as collisions caused by different velocity lags between particles with different values of $W/C_D A$, can also cause agglomeration. These effects can be described by an analysis of the particles' history; rough calculations indicate that here, too, the collision rate is small. In any case, if the particles are sufficiently small with respect to λ, then $k_{\lambda,c}$ is insensitive to the particle size (except for the effects on the conduction electrons).

The tendency of the carbon particle mass fraction to remain unchanged in the diverging section allows one, by observing the different motors successively, to measure the temperature dependence of the carbon particle

absorption coefficient, $k_{\lambda,c}$, for a given mass fraction of solid (provided that the O/F ratio can be accurately reproduced). Thus both the temperature and wavelength dependence of $k_{\lambda,c}$ can be obtained without knowing the density of the carbon cloud. We do not obtain the absolute value of $k_{\lambda,c}$; however, it is the product of k_c and y_c, the particle mass fraction, which determines the radiative heat transfer at the wavelengths of interest. For a given engine this product can be measured at the exit plane, and a flow field model, together with the temperature dependence of $k_{\lambda,c}$, allows extrapolation of it to other parts of the plume.

The temperature at the exit plane of each motor is measured by means of a spectral absorption-emission technique.[18] By such a measurement at 4.4 μ, where the emission is produced by the CO_2 and CO vibration-rotation bands, one obtains the gas temperature. By a measurement in the molecular "window" at 2.2 μ, one obtains the carbon particle temperature. In all our measurements, these temperatures were never different by more than the estimated error in each. This result is expected[19] if the particle diameter is sufficiently small. The gaseous composition is determined from a thermochemical calculation using the experimental P_c, P_e, and O/F ratio.

In Fig. 7 we show the measured exit temperature of the 5.25:1 engine as a function of O/F ratio. The solid curves are the calculated frozen and shifting equilibrium exit temperatures where P_e = 1 atm. Solid carbon was not included in this calculation. At mixture ratios above 1.7, the

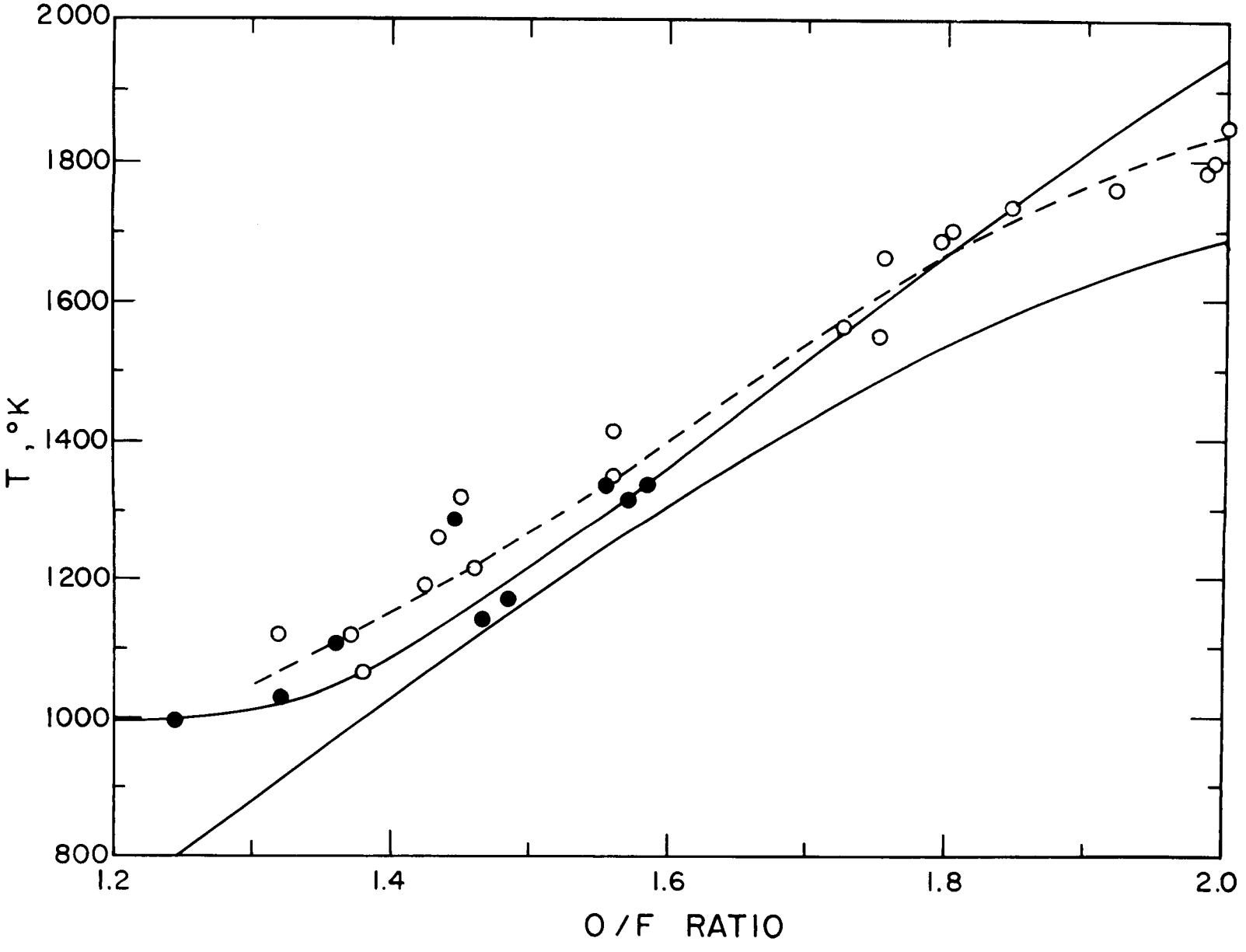

Figure 7. Exit temperatures of the 5.25:1 engine as a function of O/F ratio when P_e = 1 atm. Open points, gas temperature; solid points, carbon particle temperature. Solid lines are theoretical curves for shifting equilibrium and frozen equilibrium. Dotted line is a visual fit to data points.

measured temperatures fall between the two curves and are in fair agreement with a finite-rate nozzle flow calculation. At richer mixture ratios, there is a tendency for the measured temperatures to be greater than the calculated equilibrium values. The behavior of the T vs O/F ratio curves for the 3:1 and 1.5:1 engines is similar. A similar phenomenon was reported by Simmons[20,21] and by Hoglund, Carlson, and Byron.[22] In our case, we do not appear to have the delayed combustion or the carbon-rich hot boundary layers postulated by these investigators. Here a possible explanation of the high exhaust temperatures may be found in the influence of carbon formation on the exhaust gas thermochemistry. The reactions

$$2\ CO \rightarrow CO_2 + C(s)$$

and

$$CO + H_2 \rightarrow H_2O + C(s)$$

are exothermic by about 50 kcal. The energy released by producing carbon (at rich conditions) in the combustion chamber, assuming that the gaseous products attain equilibrium among themselves, is enough to explain the observed temperatures. In Fig. 8 we show, as a function of O/F ratio, the mass fraction of C(s) which is sufficient to explain the observed temperatures in Fig. 7 for both equilibrium and for frozen flow. A similar behavior is found for the temperature of the 3:1 and 1.5:1 engines. In Fig. 9, the measured temperatures for the three engines are plotted as a function of the mixture ratio.

From the measured spectral radiance and temperature, the spectral emis-

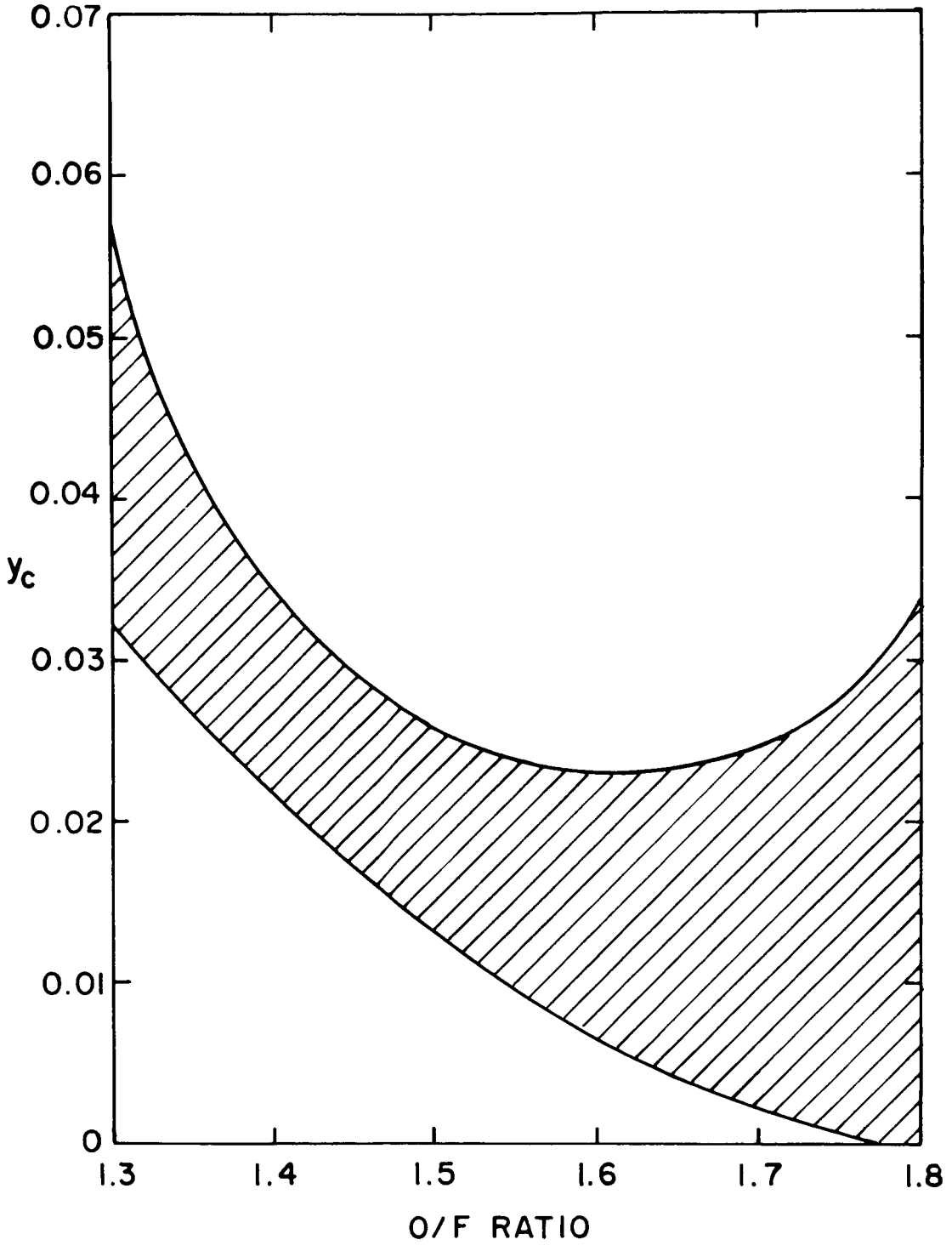

Figure 8. Mass fraction of solid carbon which could account for observed exit temperatures. Upper curve, frozen flow; lower curve, shif equilibrium flow of gas.

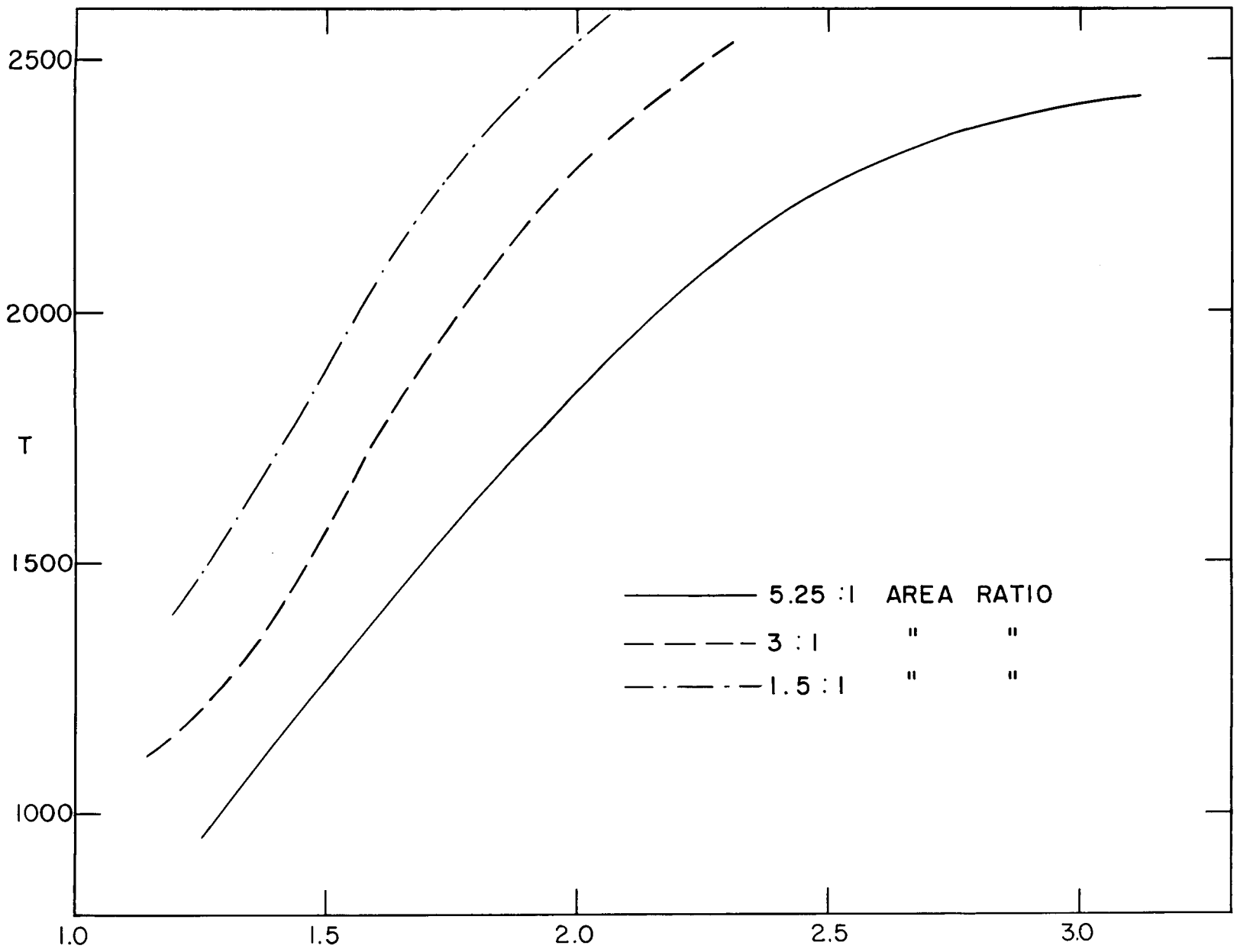

Figure 9. Temperature versus O/F ratio for the three engines.

sivity ϵ_λ of the gas-particle mixture is determined. The contribution to ϵ_λ from the gaseous emitters (H_2 and CO_2) is known as a function of temperature from previous measurements.[15,23-25] The product of the spectral absorption coefficient of carbon and carbon mass density can be obtained from

$$k_{\lambda,c}\ \rho_c = \frac{1}{\ell}\left\{-\ell n\ (1-\epsilon_\lambda)-\bar{k}_{H_2O}\ u_{H_2O}-\bar{k}_{CO_2}\ u_{CO_2}\right\} .$$

In the statistical band model, the expression for the contribution of water becomes

$$\bar{k}_{H_2O}\ u_{H_2O} = uk\ (1-uk/4\bar{a})^{-\frac{1}{2}},$$

where the fine structure term is given by

$$\bar{a} = \frac{\gamma^o}{d}\sqrt{\frac{300}{T}}\ p_T\left[c_{H_2O}\left(\sqrt{\frac{300}{T}}+\sigma\right)(1-c_{H_2O})\sigma_x\right] .$$

The concentration of the water vapor c_{H_2O} was calculated. It changes from $\sim$ 10% at a mixture ratio of 1.2 to $\sim$ 30% at a mixture ratio of 2.0. The set of absorption coefficients of water vapor was given elsewhere.[26]

The concentration of CO_2 ranges from $\sim$ 5% to 9% in the mixture ratio range from 1.2 to 2.0. It can be shown that under the present conditions Beer's law applies; thus, $\bar{k}_{CO_2} = S/d$, where S/d as a function of wavelength and temperature was given by Malkmus.[27]

If the carbon particle diameter d_p is comparable to λ, scattering as well as emission and absorption may affect the observed radiance (and the

base heat transfer). In general, the effect of scattering will be to reduce the total energy radiated by the plume. The radiation in particular directions and the local flux in some regions may actually be enhanced, at the expense of the radiation in other directions, for some flow field configurations. Carbon particles were collected on small water cooled plates passed rapidly through the exhaust jet at about 4 inches downstream from the exit plane, where the mixing layer, in which the afterburning occurs, is still thin. The flat brass plates were polished, and a carbon film with an average grain size of 20 Å was deposited. After the plates were passed through the exhaust plume, the carbon film together with the plume deposits was separated from the plates and stereographic photomicrographs with shadow casting (under an elevation angle of 25°) were made. In Figs. 10-13, we show the samplings taken at mixture ratios of 1.8 and 2.0. These samplings were only successful at a mixture ratio of > 1.6 since at lower mixture ratios the deposits were too heavy and the particles agglomerated so much that no individual particles were discernible. The agglomerations observed in the figures can be formed either during combustion and in the expanding gas or during collection on the plates. In the first case, i.e., the small carbon particles are already agglomerated in the exhaust gas, light could be scattered for $\lambda > 1\ \mu$. However, we believe that the agglomeration takes place during the collecting process. The mean value of d_p for the collected particles, which are expected to be among the larger particles in the flow (since only these possess enough momentum to cross the flow streamlines about the collector), is 400 Å. Particles of this size are not expected to scatter infrared radiation appreciably; when $\lambda < 1\ \mu$, the observed spectral radiance might be affected by scattering. However,

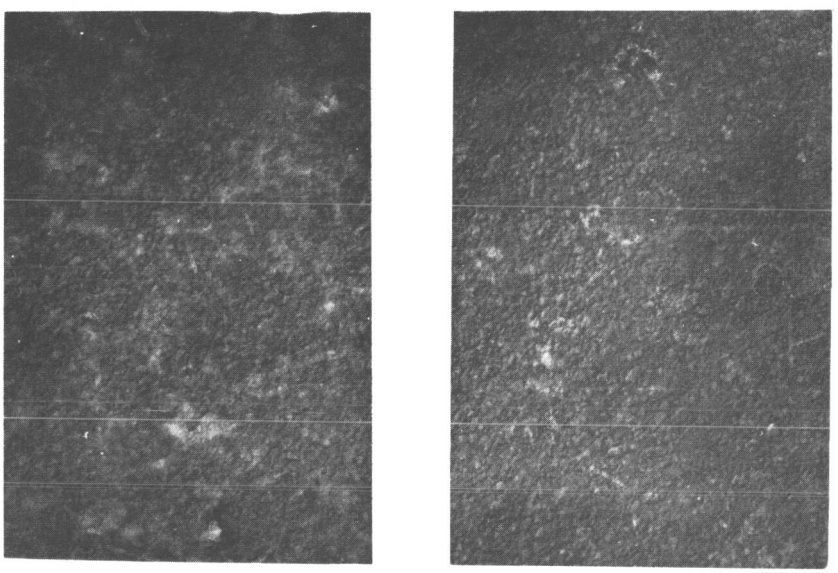

Figure 10. Photomicrograph of carbon film background. Magnification of 25,000.

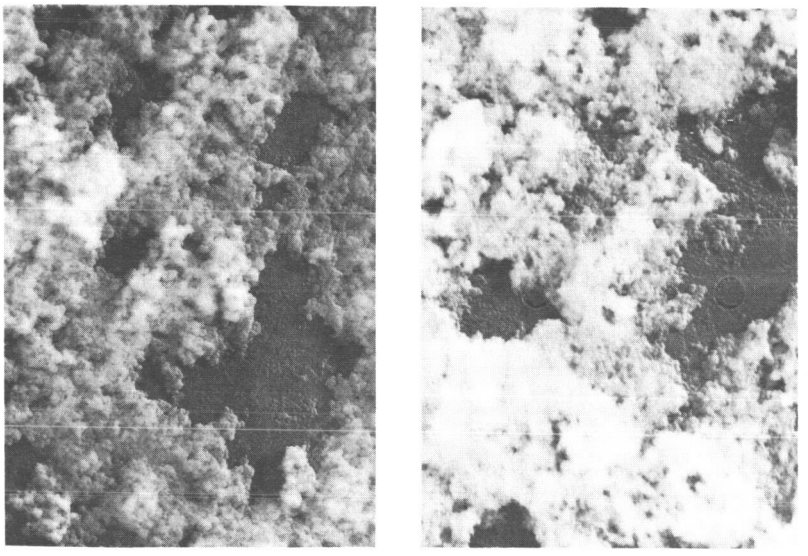

Figure 11. Photomicrograph of carbon sampling at an O/F ratio of 1.8. Both pictures are made with wide objective aperture at 75 keV (left) and 100 keV (right) with a magnification of 5,500. Shadow casting.

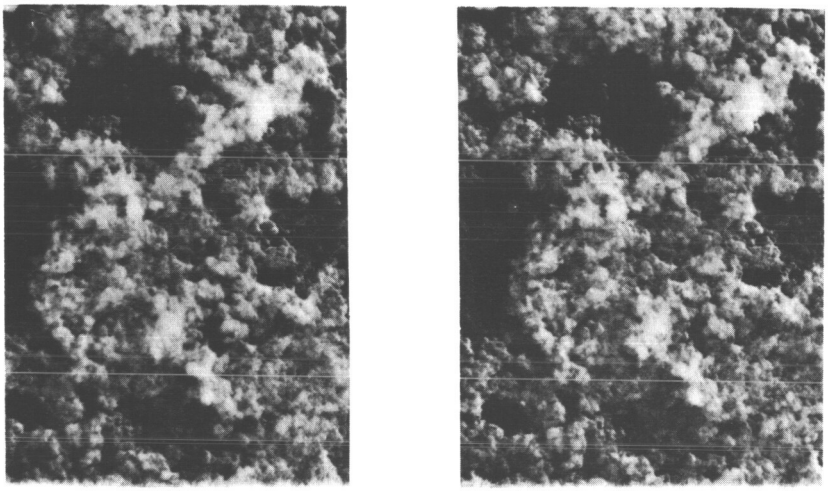

Figure 12. Stereographic photomicrograph of carbon sampling with shadow casting at an O/F ratio of 1.8. Magnification of 25,000, i.e., 0.1" = 1270 Å.

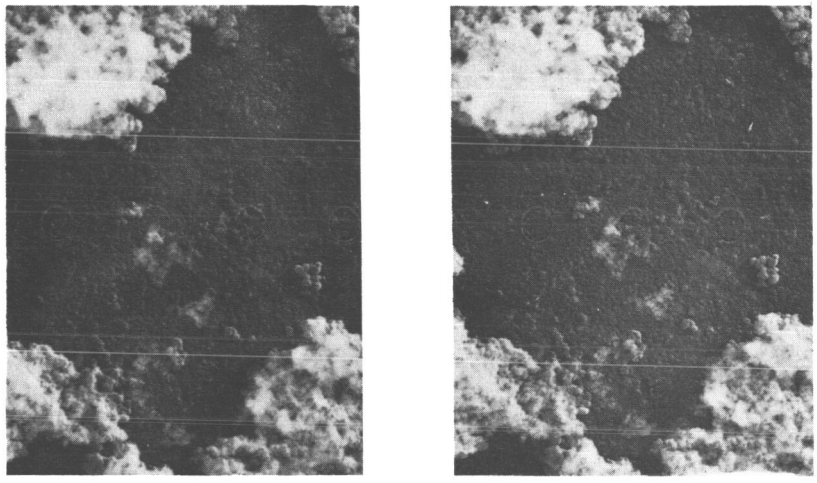

Figure 13. Stereographic photomicrograph of carbon sampling with shadow casting at an O/F ratio of 2.0. Magnification of 20,000, i.e., 0.1" = 1000 Å.

scattering should contribute a negligible amount to the radiative base heat transfer, which is only significant for $\lambda > 1\ \mu$. The results of this study are in good agreement with previous measurements made on an engine similar to that used here.[29]

When $P_e \neq P_a$, as was the case for the 3:1 and 1.5:1 motors, the possibility of a nonuniform condition along the line of sight exists. Immediately downstream of the exit plane, the gas undergoes a Prandtl-Meyer expansion when $P_e > P_a$. For the 3:1 and 1.5:1 engines the expanded regions contribute less than 5 and 10 percent, respectively, to the absorption along an optical path 2 mm downstream from the exit plane. Our measurements were made within this region, and the effects of unbalance were therefore negligible in this experiment. A photograph of the exit flow at an exit pressure of 2 atm (3:1 engine) is shown in Fig. 14.

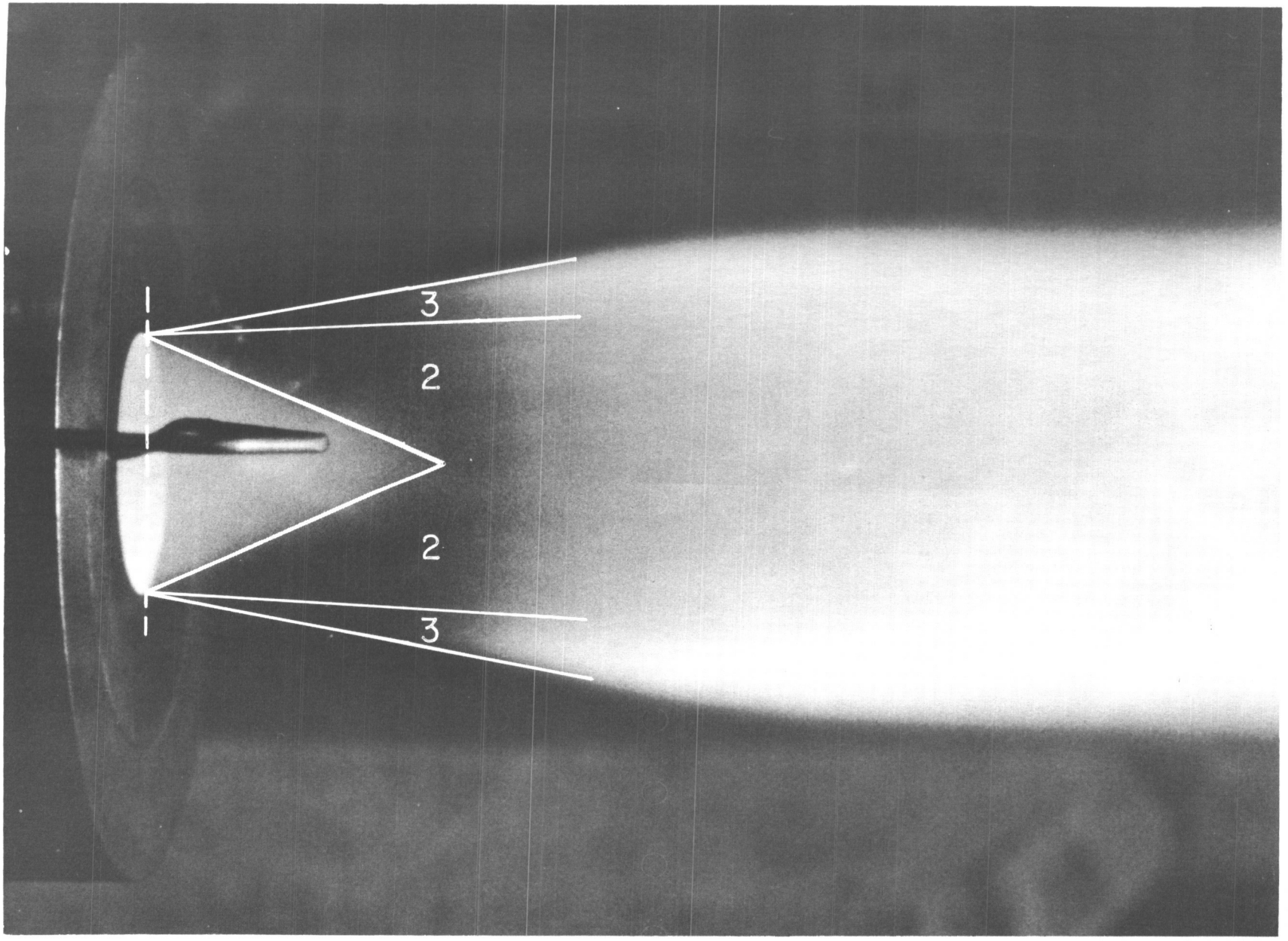

Figure 14. Photograph of the exit flow at an exit pressure of 2 atm. Region 1 is the undisturbed cone, region 2 is the Prandtl-Meyer expansion zone, and region 3 is the mixing zone. The spectrometer line of sight is indicated by a dotted line.

EXPERIMENTAL RESULTS

The carbon particle absorption coefficients ($k_{\lambda,c} y_c$) deduced from our measurements are shown in Figs. 15, 16, and 17. The theoretical calculation (matched to the experiment at $\lambda = 2.2\ \mu$) is also shown. Measurements were made outside the range of data shown, but their error limits are high. At wavelengths shorter than 1.5 μ, small errors in temperature are the principal error source (particularly at low temperatures) when measurements are made in emission. Absorption measurements are subject to large subtraction errors when absorption is low - i.e., when y_c is small. At wavelengths longer than 4 μ, the continuum emission is masked by the strong 4.3-μ band of CO_2, the 4.6-μ band of CO, and the 6.3-μ band of H_2O. A lower limit is placed on the temperature by the necessity for smooth operation of the rocket and by the heating loads which the monochromator housing can tolerate. At O/F ratios below about 1.2, the heating from the afterburning plume is severe. An upper limit to temperature arises from the requirement that the continuum emission be a reasonable fraction of the total at a given wavelength and above the instrumental noise level. At O/F ratios greater than about 2.0, the engines used produce only very small amounts of carbon.

Although the range of the data is therefore limited, some conclusions can be drawn about the behavior of carbon from our engine in the wavelength regime most important to the base heating problem. It appears that the dependence of $k_{\lambda,c}$ on λ is reasonably similar in calculation and experiment for temperatures $\leq 1700°K$. This agreement is not necessarily expected, since it is by no means clear that the rocket soot is at all like bulk

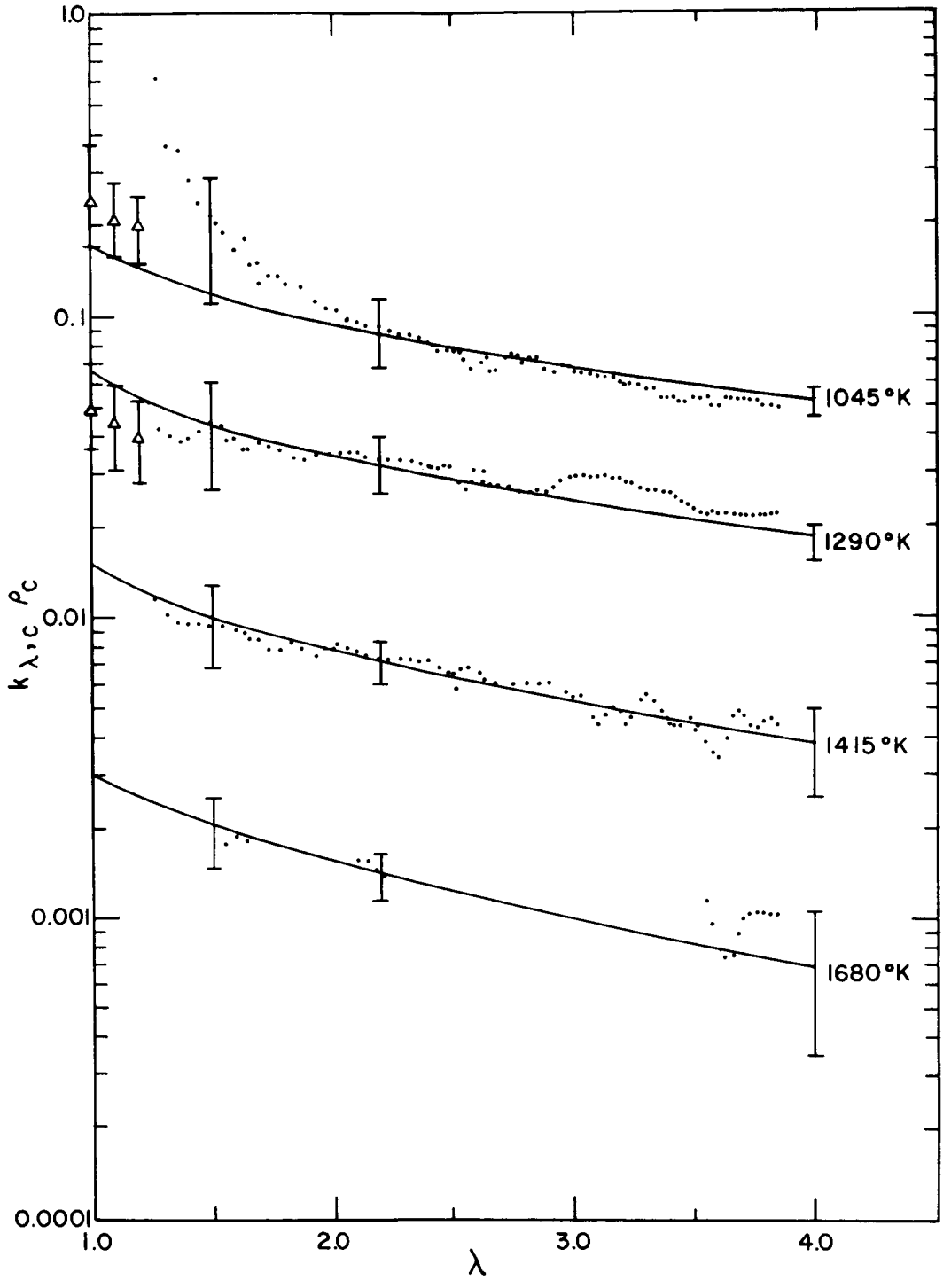

Figure 15. Values of $k_{\lambda,c}\rho_c$ determined from measurements on the 5.25:1 motor. Dots are experimental values measured in emission, triangles are values measured in absorption, solid line is theoretical calculation based on bulk carbon properties.

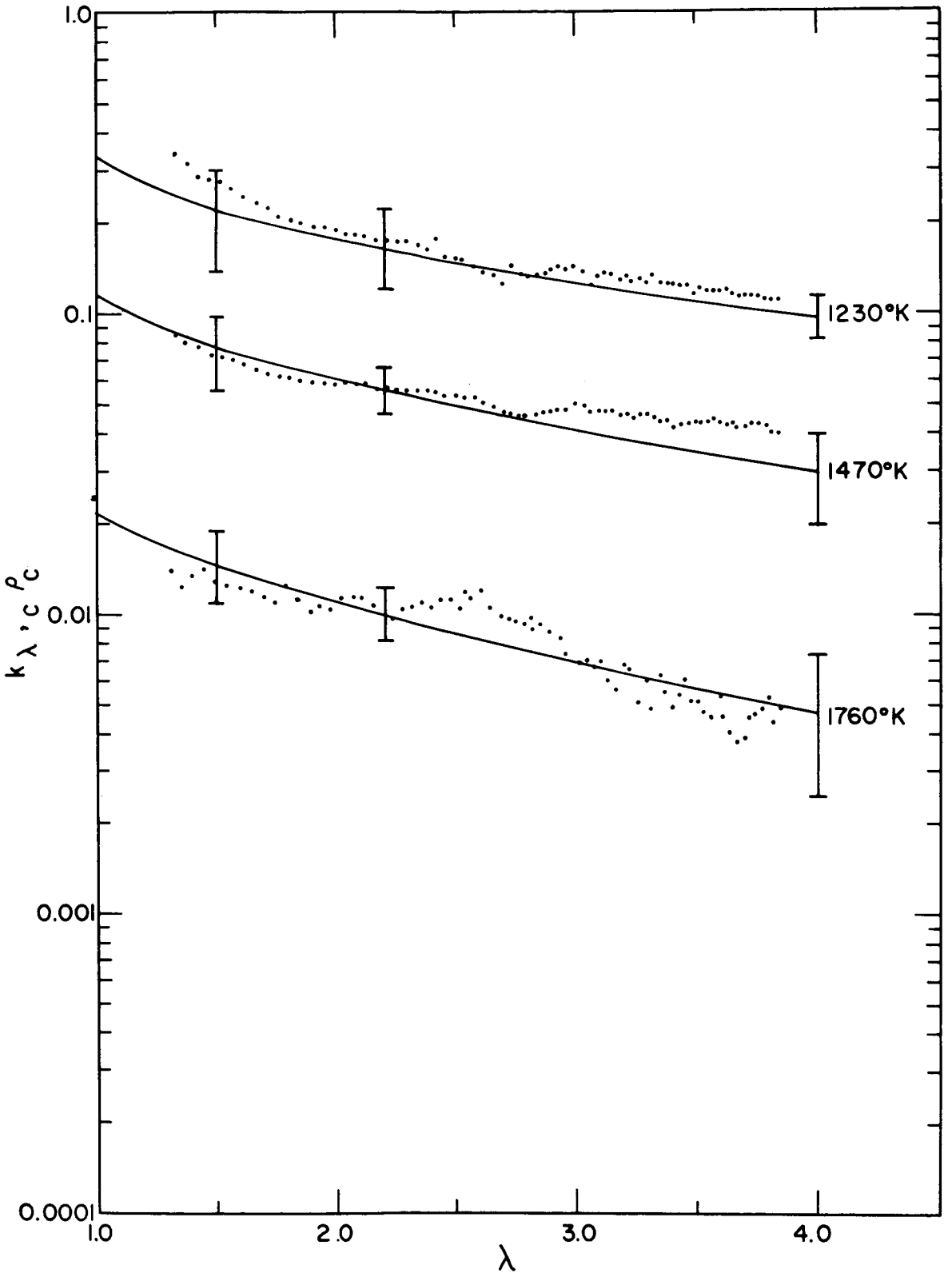

Figure 16. Values of $k_{\lambda,c}\rho_c$ determined from measurements on the 3:1 motor.

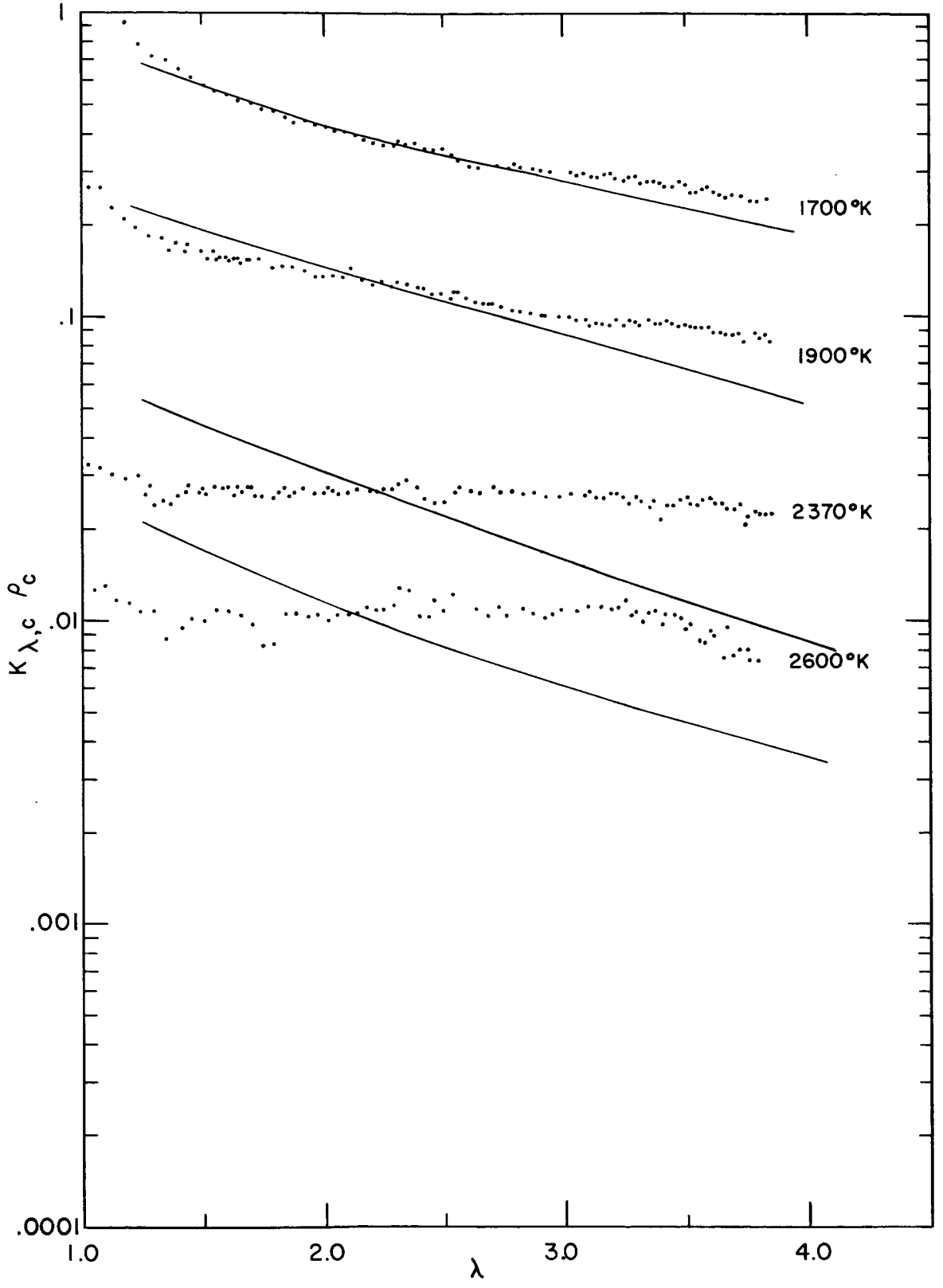

Figure 17. Values of $k_{\lambda,c}\rho_c$ determined from measurements on the 1.5:1 motor.

carbon. The agreement between the experimental and calculated spectral dependence is comparable to that shown for soot from laboratory flames in Fig. 4, though it has been demonstrated over a smaller spectral region. A spectral variation of $k_{\lambda,c}$ as λ^{-1}, which has sometimes been proposed for soot in flames, is also consistent with our data at these lower temperatures. Since a rocket burns a spray of liquid fuel droplets at high pressure, and a laboratory flame burns gases at low pressure, one would not necessarily have expected this agreement either. At temperatures > 1700°K the experimental data are markedly different from the theoretical values and appear to be almost independent of wavelength.

At short wavelengths and low temperatures, there is a discrepancy between the results of emission and absorption measurements, with the values of $k_{\lambda,c}$ determined in absorption being lower and closer to the calculated curve. In fact, at temperatures below 1200°K, the observed emitted intensity at $\lambda < 0.8\ \mu$ is greater than the blackbody intensity at the measured temperatures. Transmission measurements made in this temperature and wavelength region result in apparent absorptivities considerably less than the apparent emissivities. The difference is too large to be explained by an error in temperature measurement. Possible explanations include (1) a nonequilibrium distribution of emitting states in the gas, and (2) the presence of scattered radiation from some other, hotter, part of the flow field.

An indication that scattering plays a role in the emission from carbon-rich exhaust jets at the shorter wavelengths was obtained from an experiment in which a "sun gun" lamp with a tungsten filament at 3200°K

was placed next to the rocket exhaust perpendicular to the monochromator line-of-sight. An appreciable increase in signal was obtained with the lamp over that recorded without it. However, in this crude experiment, it was not possible to measure accurately the spectral dependence of the scattered signal. The effects of scattering at short wavelengths may explain the unusually high emission observed by Simmons in his vernier experiment when $\lambda < 1\ \mu$.

A comparison of the theoretical and experimental values of radiant intensity can be used to determine the effect of chamber pressure upon the apparent mass fraction of carbon produced by these engines. Using the 3:1 engine, the exit temperature and continuum emission level were measured at P_c's between 15 and 60 atm. The results, shown in Fig. 18, indicate that y_c is increased by increasing chamber pressure.

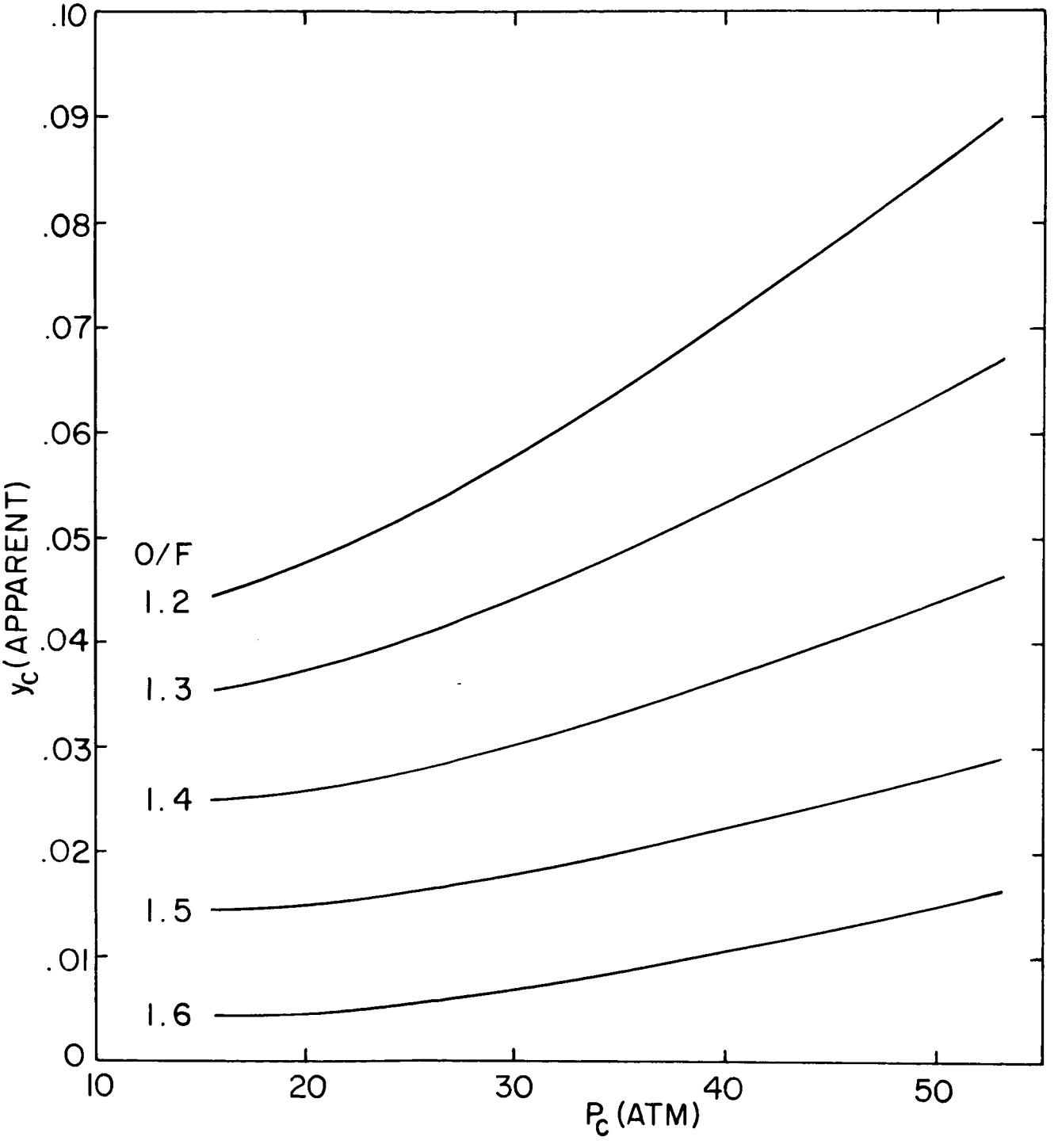

Figure 18. Dependence of apparent value of y_c on chamber pressure at different O/F ratios.

DISCUSSION

The experimental and calculated spectral dependences of $k_{\lambda,c}$ agree at temperatures below 1700°K. The temperature dependence of $k_{\lambda,c}$ in this range can be ascertained in the following manner: If the calculation correctly predicts the temperature dependence, values of the carbon mass fraction y_c deduced from the measured value of $k_{\lambda,c}y_c$ for the different engines at the same operating conditions by comparison with the calculation should be the same. If there is a significant difference between calculation and experiment, then the values of y_c computed in this manner will differ.** Carbon mass fractions determined from the experimental results and the calculation at 2.2 μ are shown in Fig. 19 as functions of O/F ratio. The errors in y_c as a result of uncertainties in temperature and radiance measurements, and in O/F ratio as a result of propellant metering errors, are also shown. There appears to be no definite tendency of y_c's determined from any engine to be consistently above or below those from the others, and the error bounds overlap to a large degree. The calculated temperature dependence of y_c is therefore consistent with the measured data below 1700°K. (On the other hand, the calculated variation in $k_{\lambda,c}$ at 2.2 μ between 1000° and 1700°K is only 25%, and almost as good agreement could have been obtained by assuming no dependence of $k_{\lambda,c}$ on temperature in this range.)

At temperatures greater than 1700°K, the lack of agreement between calculated and observed spectral dependence of $k_{\lambda,c}$ indicates that, at least for some wavelengths, the calculated temperature dependence must also

---

** Assuming that no change in y_c in the divergent section occurs.

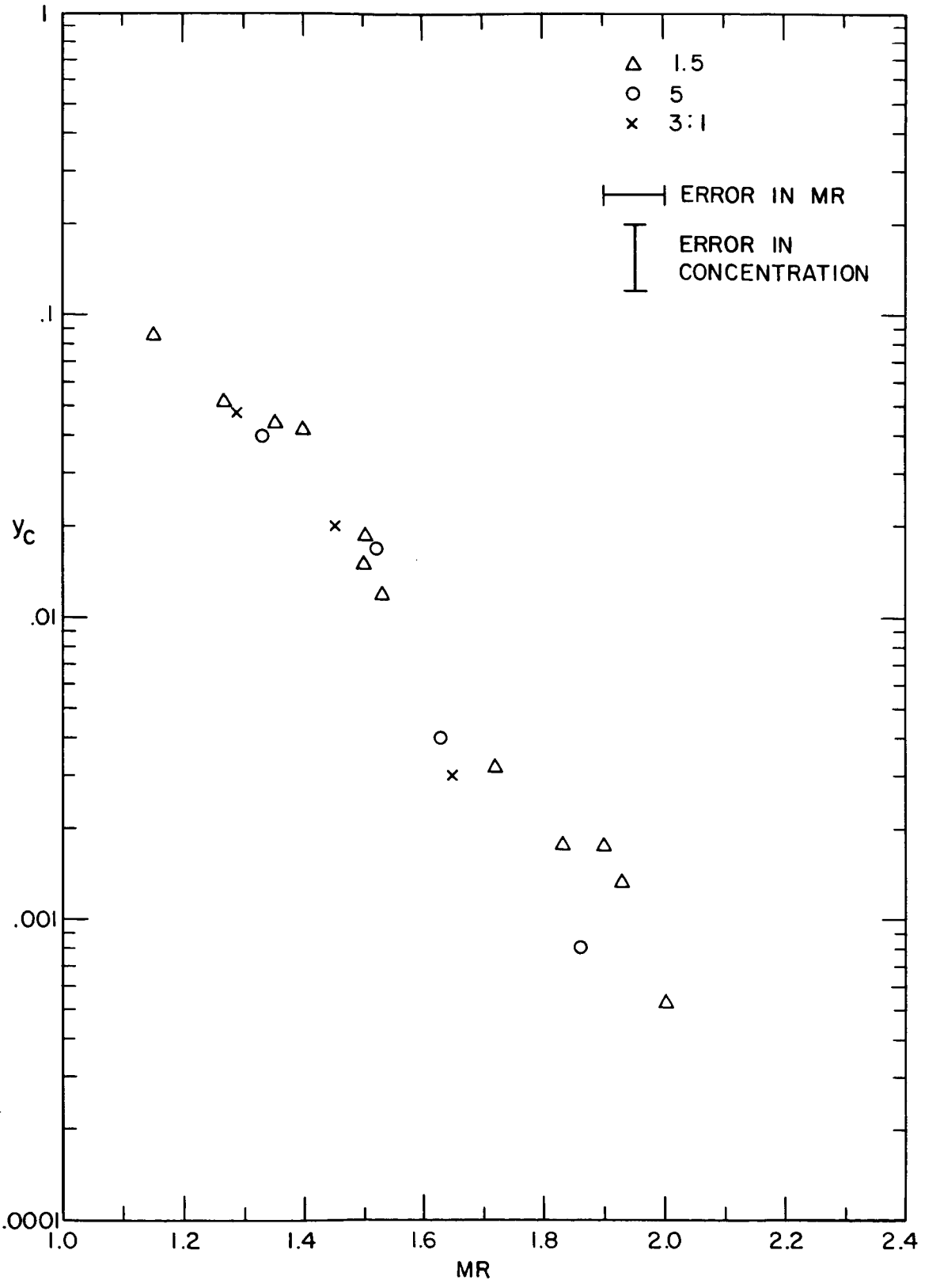

Figure 19. Carbon mass fraction versus O/F ratio.

disagree with the experimental results. At 2.2 μ, the values of y_c determined as before for temperatures above 1700°K, do not agree with those determined for lower temperatures. However, at approximately 1.0 μ, the agreement of y_c's from high and low temperature results is reasonably good.

Empirical values of $k_{\lambda,c}$ have been deduced from the low-temperature values of y_c and the high-temperature values of $k_{\lambda,c}y_c$, in order to provide a set of absorption coefficients consistent with our data over the temperature range from 1000° to 2600°K. In Fig. 20 we show the resulting temperature dependence of $k_{\lambda,c}$ at selected wavelengths; the calculated temperature dependence is shown for comparison. The absorption coefficients are shown as functions of wavelength at various temperatures in Fig. 21. This figure was constructed by cross-plotting the data shown in Fig. 20; its consistency with the experimental results is shown in Fig. 22.

The empirical absorption coefficients of carbon formed by our rocket motors are listed in Table II. The high-temperature values depend on the accuracy of the apparent carbon mass fraction deduced from the lower-temperature results, and the resulting uncertainty is as much as ± 50% at the highest temperatures. The values of $k_{\lambda,c}$ given in Table II are those which best fit our experimental data; their use in base heating calculations is recommended.

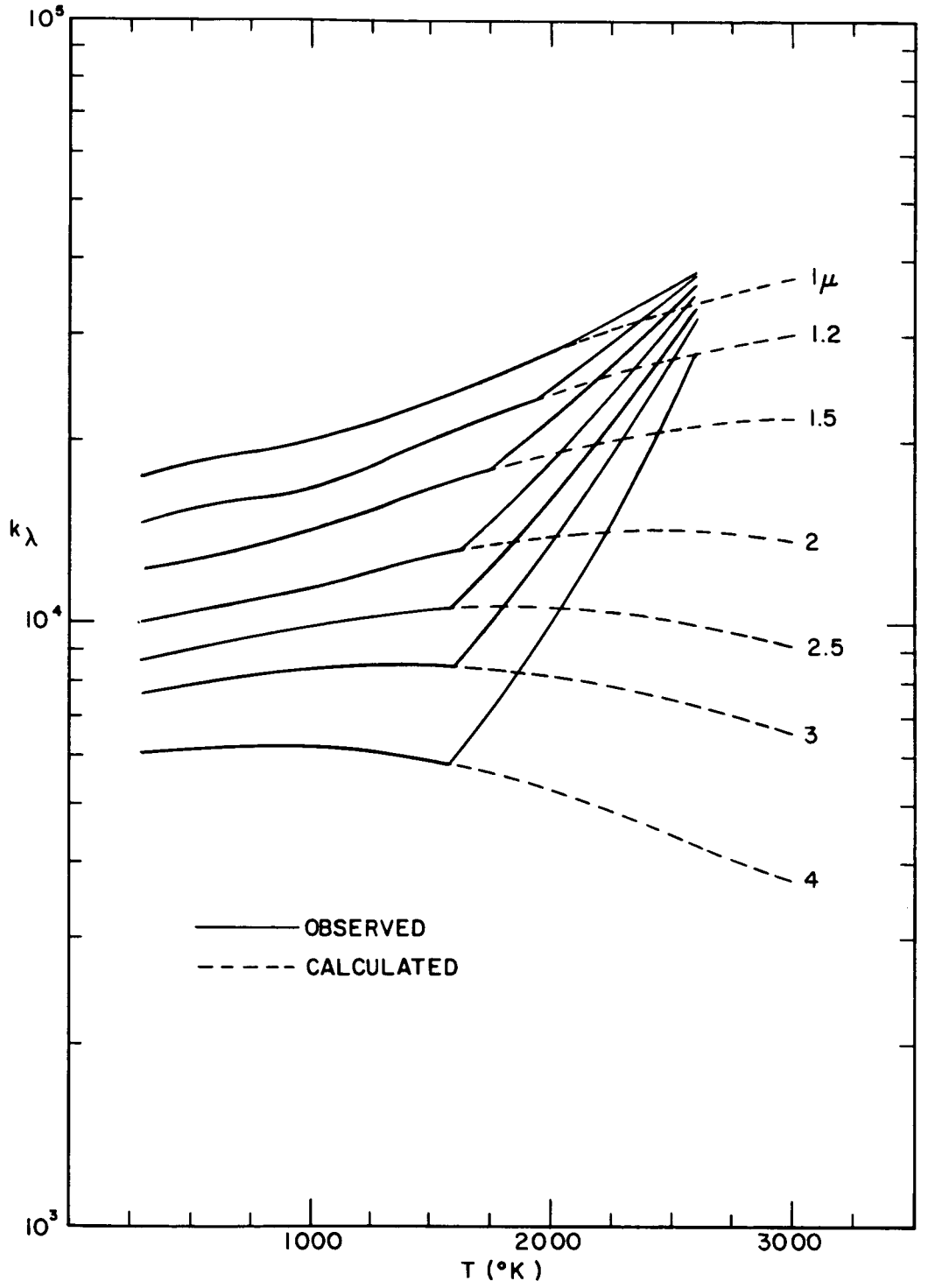

Figure 20. Absorption coefficients versus temperature for different wavelengths. Theoretical values are represented by solid line, experimental values are shown in dashed lines. At the lower end of the temperatures, both values are the same.

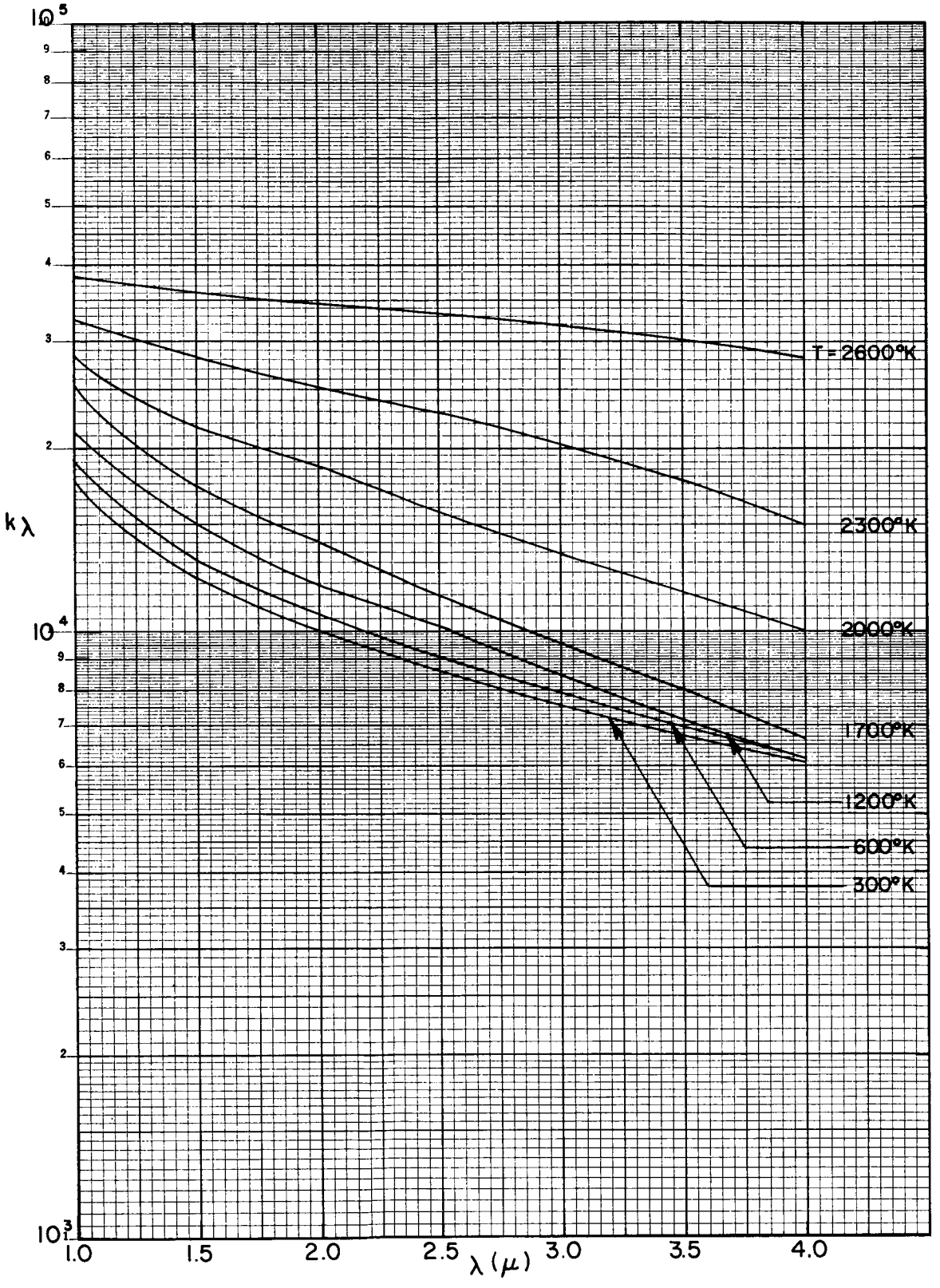

Figure 21. Absorption coefficients versus wavelength for different temperatures. This is a cross plot of Fig. 20, using the values consistent with the experimental data.

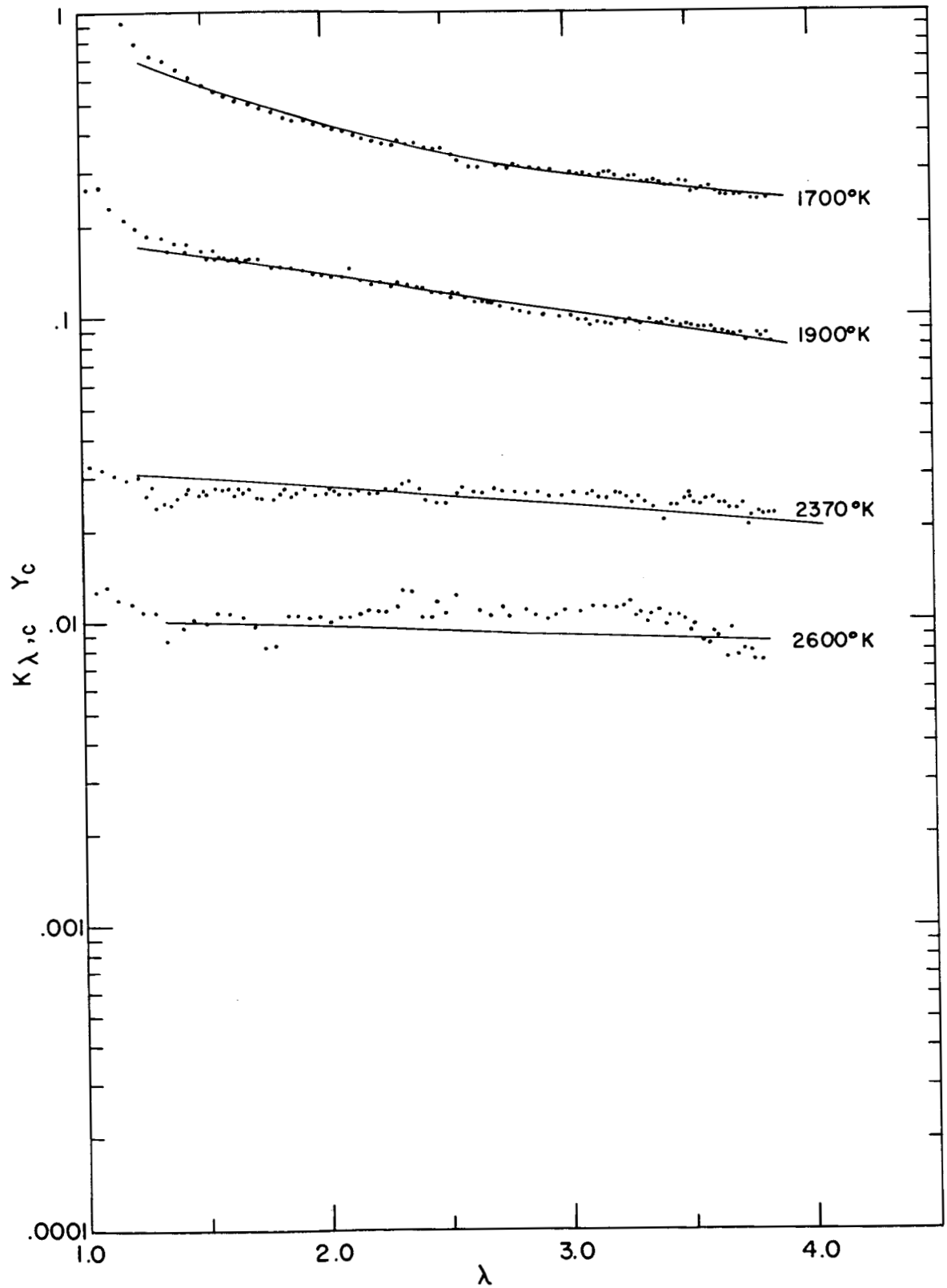

Figure 22. Comparison of experimental data with the set of absorption coefficients given in Fig. 21 and Table II.

TABLE II

ABSORPTION COEFFICIENTS FOR CARBON (SQ.CM/GM)

1/CM	300.K	600.K	1200.K	1700.K	2000.K	2300.K	2600.K
2500.0	.610E 04	.615E 04	.611E 04	.669E 04	.100E 05	.151E 05	.282E 05
2750.0	.655E 04	.678E 04	.690E 04	.765E 04	.113E 05	.171E 05	.298E 05
3000.0	.700E 04	.730E 04	.760E 04	.850E 04	.122E 05	.187E 05	.308E 05
3333.3	.763E 04	.800E 04	.851E 04	.955E 04	.135E 05	.204E 05	.320E 05
3636.4	.810E 04	.850E 04	.932E 04	.105E 05	.145E 05	.218E 05	.328E 05
4000.0	.860E 04	.920E 04	.103E 05	.116E 05	.157E 05	.230E 05	.330E 05
4444.4	.925E 04	.983E 04	.111E 05	.127E 05	.172E 05	.240E 05	.340E 05
5000.0	.100E 05	.107E 05	.119E 05	.141E 05	.186E 05	.251E 05	.348E 05
5714.3	.110E 05	.118E 05	.133E 05	.155E 05	.200E 05	.267E 05	.352E 05
6666.7	.123E 05	.131E 05	.151E 05	.173E 05	.218E 05	.280E 05	.360E 05
8333.3	.146E 05	.157E 05	.182E 05	.210E 05	.250E 05	.305E 05	.374E 05
10000.0	.175E 05	.188E 05	.211E 05	.251E 05	.281E 05	.325E 05	.380E 05

CONCLUSION

At temperatures between 1000° and 1700°K, the spectral dependence of carbon particle cloud absorption coefficients measured in the exhaust gases from small rocket engines are in reasonably good agreement with the results of a calculation based on the properties of bulk carbon for wavelengths between 1.0 and 4.0 μ. A spectral variation of $k_{\lambda,c}$ as λ^{-1} is also compatible with these data, and the predicted temperature dependence is less than the error limits of the experiment.

At temperatures greater than 1700°K, the experimental and theoretical spectral dependence diverge. The present experimental data were used to deduce absorption coefficients between 1700° and 2600°K.

There is no large difference apparent at temperatures below 1700°K between the optical properties in the near infrared of the carbon formed in laboratory flames and in our small research engine. Deviations between calculation and experiment at shorter wavelengths appear to be caused by scattering processes peculiar to the observed flow system. Similar effects should be expected to appear in other measurements of exhaust emission at short wavelengths, and some caution should be employed in interpreting them.

Careful measurements of continuum emission in large engines are necessary before these conclusions can be generalized to include them.

REFERENCES

1. W. F. Rector, III, "Evaluation of Heating to the Aft Heat Shield on the XSM-65 Missile Based on "B" Series Flight Test Data," GD/C Report ZJ-7-062 TN, October 1958.
2. S. S. Penner, M. Thomas, and G. Adomeit, "Similarity Parameters for Reacting Multicomponent Gas Mixtures with Radiative Energy Transfer," Calif. Inst. Tech. Report 7 (AFOSR 2578), May 1962.
3. "Scaling of Rocket Motor Exhaust Optical Radiation," General Dynamics/ Convair Report GDA-63-0507, SSD-TDR-63-188, July 1963.
4. H. C. Hottel, "Radiant Heat Transmission," in Heat Transmission by W. H. McAdams (McGraw-Hill Book Co., New York, 1954), pp. 99-105.
5. A. G. DeBell and E. W. Speiser, "Infrared Spectral Radiance of Large Liquid Propellant Rocket Engine Exhaust Plumes," Rocketdyne Report R-2019, AFCRC-TR-60-226, April 1960.
6. A. G. Gaydon and H. G. Wolfhard, Flames: Their Structure, Radiation, and Temperature (Chapman and Hall, Ltd., London, 1953).
7. H. C. Hottel and F. P. Broughton, "Determination of True Temperature and Total Radiation from Luminous Gas Flames," Ind. Eng. Chem. 4, 166-75 (1932).
8. Eighth Symposium (International) on Combustion (The Williams and Wilkins Co., Baltimore, 1962), pp. 784-814 (papers 84-87).
9. R. C. Millikan, "Measurement of Particle and Gas Temperature in a Slightly Luminous Premixed Flame," J. Opt. Soc. Am. 51, 535-42 (1961).
10. R. G. Siddall and I. A. McGrath, "The Emissivity of Luminous Flames," Ninth Symposium (International) on Combustion (Academic Press, New York, 1963), pp. 102-110.

11. P. J. Foster, "Calculation of Optical Properties of Dispersed Phases," Combustion and Flame 7, 277-82 (1963).

12. V. R. Stull and G. N. Plass, "Emissivity of Dispersed Carbon Particles," J. Opt. Soc. Am. 50, 121-129 (1960).

13. F. S. Simmons, "The Spectral Emissivity of Dispersed Carbon in Rocket Exhaust Gases," Rocketdyne Research Report 60-14, June 1960.

14. H. Senftleben and E. Benedikt, "Diffraction of Light by Carbon Particles of Luminous Flames," Annalen Der Physik, 4th Ser., 60, 297-323 (1919).

15. C. C. Ferriso and C. B. Ludwig, "Spectral Emissivities and Integrated Intensities of the 2.7-μ CO_2 Band between 1200° and 1800°K," J. Opt. Soc. Am. 54, 657-62 (1964).

16. K. Foelsch, "The Analytical Design of an Axially Symmetric Laval Nozzle for a Parallel and Uniform Jet," J. Aero. Sci. 16, 161-166 (1949).

17. H. L. Green and W. R. Love, Particulate Clouds: Dusts, Smokes, and Mists (D. von Nostrand Company, Inc., London, 1957), pp. 128-131.

18. S. Silverman, "The Determination of Flame Temperature by Infrared Radiation," J. Opt. Soc. Am. 39, 275-77 (1949).

19. F. S. Simmons and F. G. Spadaro, "Thermal Lag of Solid Particles in Rocket Nozzle Flow," Rocketdyne Research Rept. No. 59-27, 1959.

20. F. S. Simmons, "Expansion of Liquid-Oxygen/RP-1 Combustion Products in a Rocket Nozzle," ARS J. 30, 193-94 (1960).

21. F. S. Simmons and A. G. DeBell, "Spectral Radiometry and Two-Path Pyrometry of Rocket Exhaust Jets," Rocketdyne Research Report RR-61-9, 1961.

22. R. Hoglund, D. Carlson, and S. Byron, "Experiments on Recombination Effects in Rocket Nozzles," AIAA J. 1, 324-29 (1963).

23. C. C. Ferriso, "High-Temperature Spectral Absorption of the 4.3-Micron CO_2 Band," J. Chem. Phys. 37, 1955-61 (1962).

24. C. C. Ferriso and C. B. Ludwig, "Spectral Emissivities and Integrated Intensities of the 2.7-μ H_2O Band between 530° and 2200°K," J. Quant. Spectry. Rad. Transfer 4, 215-27 (1964).

25. C. C. Ferriso and C. B. Ludwig, "Spectral Emissivities and Integrated Intensities of the 1.87-, 1.38-, and 1.14-μ H_2O Bands between 1000° and 2200°K," J. Chem. Phys. 41, 1668-74 (1964).

26. C. C. Ferriso, C. B. Ludwig, and A. Thomson, "Empirical Infrared Absorption Coefficients of H_2O from 300°K to 3000°K," General Dynamics/ Convair Report No. GD/C-DBE65-028, December 1965.

27. W. Malkmus, "Infrared Emissivity of Carbon Dioxide (2.7-μ Band)," J. Opt. Soc. Am. 54, 751 (1964).

28. F. P. Boynton, "Rocket Plume Radiance. IV. Studies of Carbon Particles Formed by Small Hydrocarbon-Fueled Rocket Engines," General Dynamics/ Convair Report ERR-AN-007, 7 April 1960.